6 RESULTS

With the aim of better understanding the process of instability development in the operating region of the point 3 test conditions of the Low Flow Stability Tests, three small pressure perturbation steam line tests (see Section 5.1 for the related specifications) have been performed. These transient perturbations have been investigated employing the coupled RELAP5 Mod3.3/PARCS code. With these codes it is possible to obtain detailed information regarding the state of the reactor at each integration time step, primarily the power distribution and the nuclear cross-section for each core nodes. Using these values, for each disturbance test, a signal modal decomposition was performed with the VALKIN code with the aim to compare the power evolution for the transient using a 3-D classical neutronic-thermalhydraulic coupled codes and a 3-D modal code. Additionally, in order to characterize the studied transient as in-phase or out-of-phase and also to study the importance of different modes during the transients, the time dependent power signal was decomposed into several harmonic contributions.

Then, several VALKIN transient calculations have been carried out with the purpose of observing the difference between the results obtained using different numbers of modes or different updating times.

Moreover, for two perturbation tests (Case A1 and Case C1), the results for the power modal decomposition have been complemented with the information provided by the simulation of the LPRM signals by RELAP5/PARCS coupled codes: a modal decomposition (with the VALKIN code) of the neutronic power from the local power distribution in the reactor core (made available by the coupling codes) was performed and the results have been compared by the information achieved from this decomposition with the one obtained from the LPRM outputs also simulated by these same coupling codes.

Finally, for each perturbation test, the Decay Ratio and the Natural Reactor Frequency have been calculated and it was analyzed the phase shift of opposite LPRM signals (given by the RELAP5/PARCS calculations) in order to examine the characteristics of the oscillations developed.

6.1 CALCULATION STEPS

6.1.1 RELAP5/PARCS Coupled Calculation

The following steps were accomplished to perform all the RELAP5/PARCS coupled calculations

1. The RELAP5 code was run stand alone for about 1000 s of steady state with the one channel nodalization and for 200 s with the 33 thermalhydraulic channels nodalization, in order to allow the parameter to reach stable values.
2. The RELAP5 and PARCS codes were then run coupled in a steady state, basically until a stability convergence value for K-effective was found.
3. The RELAP5 and PARCS codes were run coupled for a null transient to make it sure that the stable conditions exist (100 s are required to reach stable conditions if the simulation has performed with the 33 T/H channels model and 150 s if it was carried out with the single T/H channels core nodalization).
4. The RELAP5 and PARCS were run coupled to perform the several transient calculations

The results are provided also by a video clip related to the Case C1 (see the attached CD-ROM) concerning the variation during the transient time of the average power in the core.

This representation is necessary and useful in order to investigate specific and local results in such complex transient requiring a three-dimensional neutron kinetics modeling apart from the help needed to analyze the transient results and to synthesize several parameters in a single issue.

6.1.2 Decay Ratio and Natural reactor Frequency Calculation

According to all that was discussed in the section 4.6, the following steps were accomplished in order to calculate the Decay Ratio and the Natural reactor Frequency in all the perturbation tests.

In the framework of the parametric time series analysis a linear dynamical system has been set up characterized by a difference equation (or a system of difference equations) on the basis of a calculated discontinuous parameter time

series (power time series obtained from the RELAP5/PARCS calculations). The unknown coefficients of the difference equation(s) must be determined by a fitting procedure based on a maximum likelihood technique. In practice, the coefficients are obtained by minimizing the sum of the squared residuals (a step called system identification problem). Depending of the number of coefficients on the left and right hand-side of the model equation used for the identification procedure an auto-regressive (AR) or an auto-regressive moving average (ARMA) model is generated. In addition to estimating the model parameters, the determination of the model order is essential since it is used a so called plateau method for the ARMA model order estimation and an Akaike information criterion for the AR model order optimization. The decay ratio (DR) of the oscillation with the so-called natural frequency (NF) of the reactor is determined from the poles of the transfer function of the estimated linear dynamical system.

The parametric time series analysis is based on the in-house codes developed in the Universidad Politecnica of Valencia [29] and [30] which are not described in the present work.

6.1.3 Power modal analysis

In all cases it has been performed a modal analysis with the VALKIN code.

With RELAP5/PARCS coupled codes it is possible to obtain detailed information regarding the state of the reactor for each integration time step. In this way, it is possible to achieve, for each time step, the nuclear cross-sections for each core nodes that it has been used as input for the VALKIN code.

In order to observe the difference between the results obtained using different numbers of modes or different updating times, after run a steady state calculation, it has been performed several transient calculations. The process of updating the modes increases considerably the accuracy of the obtained solution but is an expensive process from the computational point of view, thus it has been necessary to find an equilibrium between the number of modes and its updating time to optimize the performance of the method.

6.1.4 Decomposition of the LPRM signals

For the Case A1 and C1, it has been complemented the results for the power modal decomposition with the information provide by the simulation of the LPRM signals by RELAP5/PARCS: it has been performed a modal decomposition of the neutronic power from the local power distribution in the reactor core (made available by the coupling codes) and it has been compared this decomposition with the one obtained from the LPRM outputs also simulated by these same codes.

The LPRM's are positioned between axial and lateral planes corresponding to the reactor discretization (nodes). The spatial location of the LPRM's across in the core is indicated in figure 3.6.

According to all it has been said in the section 4.5, for each cell, *(i,j,k)*, of the reactor core discretization, it has been considered local harmonic power modes:

$$P_{n,i,j,k} = \alpha\left(\Sigma_{f1i,j,k}\phi_{1,ijk,n} + \Sigma_{f2i,j,k}\phi_{2,ijk,n}\right) \tag{6.1}$$

For a given LPRM, l, in the axial level k_l, it has been defined the n-th modal power contribution to the LPRM as

$$LP_{n,l,k_l} = \sum_{i,j,k} P_{n,i,j,k_l} \tag{6.2}$$

where i,j sum over the adjacent nodes to LPRM l, as shown in figure 4.6, and k sums over the two axial planes containing the LPRM.

Then, supposing that the LPRM signals can be expressed as

$$LPRM_{l,k_l}(t) = \sum_{n} a_n^{k_l}(t) LP_{n,l,k_l} \tag{6.3}$$

the fast adjoint modes have been used to construct a weighting factor to obtain the power amplitudes, $a_n(t)$. For each LPRM, (l,k_l), it has been defined

$$W_{n,l,k_l} = \sum_{i,j,k} \phi^{+}_{1,ijk,n} \tag{6.4}$$

where $\phi^{+}_{1,ijk,n}$ is the average fast *n*-th mode component in cell *(i,j,k)*, and *i*, *j* and *k* sum over the adjacent nodes to LPRM *l*.

Assuming that the experimental signals $LPRM_{l,k_l}(t)$ are modeled by equation (6.3), and using the weights (6.4), for each axial level, k_l, it has been constructed the system of linear equations

$$\sum_{l} LPRM_{l,k_l}(t) W_{m,l,k_l} = \sum_{l} \sum_{n=1}^{N} a_n^{k_l}(t) LP_{n,l,k_l} W_{m,l,k_l} \qquad \text{where } m=0,...,N, \tag{6.5}$$

N being the number of considered modes for the power decomposition. Calculating the dominant Lambda modes for the steady state configurations corresponding to the analyzed cases, it is found, consecutively, the fundamental mode, two azimuthal modes and an axial mode. For a given axial level k_l it was impossible to obtain information about the axial mode. The number of modes considered is three, the fundamental, ϕ_0, and two azimuthal modes, ϕ_1 and ϕ_2 [25].

6.2 STEADY STATE RESULTS

The main parameters obtained after the "zero transient" calculations were compared with the reference plant data to make sure that the stable conditions of the chosen operational point were reached.

The list of parameters chosen for comparison covers reactor power and core inlet mass flowrate, core exit pressure, core inlet temperature, core inlet enthalpy and core average axial power distribution. Table 6-1 presents the main reactor parameters prior to its disturbance for the two adopted nodalizations, comparing them with available measured data. Figure 6.1 also compares the core average axial power distribution calculated with the 33 and 1 channel T/H model, with the reference one.

Table 6-1: Reactor main parameters prior to its disturbance

Parameters, Units	Measured	RELAP5/PARCS (33 channels)	RELAP5/PARCS (1 channel)
Core Thermal Power, MWt	1948.00	1949.00	1949.00
Reactor Flow, kg/s	5216.40	5216.33	5209.55
Core Inlet Temperature, K	543.16	543.01	542.19
Core Inlet Enthalpy, J/kg	1.1846E6	1.1839E6	1.1798E6
Pressure at Core Outlet, Pa	7.0980E6	7.0979E6	7.0978E6
Feedwater massflow, kg/s	941.22	941.22	941.22

It is possible to observe a good agreement among the calculated conditions and the measured values for the model with 33 core channels. The present differences do not affect the value of the instability analyses performed with this thermalhydraulic nodalization. In fact, it has been checked that the simulated reactor behaviour is nearly the same even if the initial conditions of the perturbation test are slightly changed.

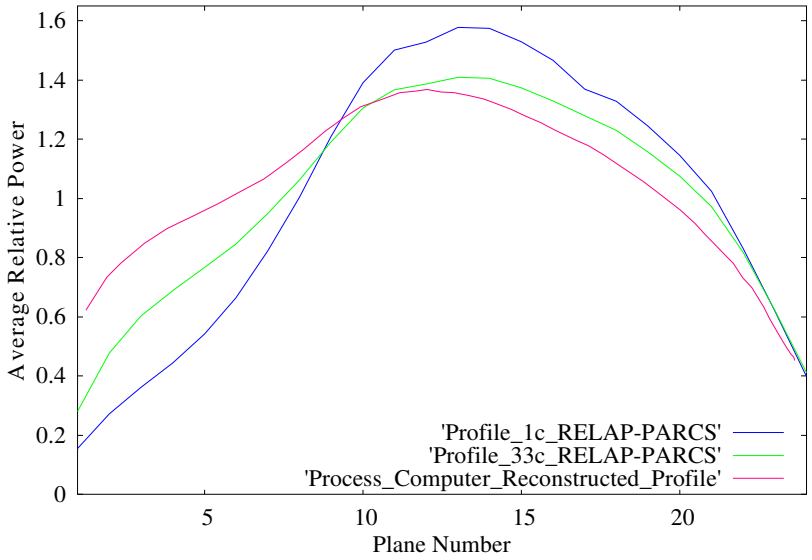

Figure 6-1: Comparison of RELAP5/PARCS calculated core average axial power distributions with experimental test (process computer corrected).

Before dealing with the analysis of the obtained results, it is important emphasize that the axial power distribution assumed as reference profile, i.e., the distribution provided in [13], has been reconstructed with a process computer from the experimental data and it is an approximation of the real average axial power profile.

Now, considering the figure 6.1, it is should be noticed that the core average axial power profile achieved in the steady state calculation by the RELAP5/PARCS coupled codes with the 33 channels model show a reasonable agreement with the reference data; on the other hand, the power distribution obtained with the single channel model, although maintains the form of the process computer reconstructed profile, differs significantly from it: in both of

cases the power is underestimated in the lower part of the core and overestimated in the middle and upper parts.

These discrepancies might be explained by the fact that the Xenon and Samarium distributions used are not the real distributions in the reactor. In fact, nevertheless the reactor conditions in the Low Flow Stability Test and in the Turbine Trip Test are comparable, the choice of using the data of the Turbine Trip Benchmark it is not completely appropriate for the poison distributions that certainly vary considerably form case to case; so, an the approximation has been introduced by this choice in the whole analysis, that can produce discrepancies between the experimental and the calculated data.

6.3 TRANSIENTS RESULTS

Six perturbation cases have been analyzed. The results of these different tests are here described in detail.

All values have been plotted in normalized form with respect to steady state values to better highlight to the behaviour of the reactor during the transient.

6.3.1 Case A: Two Peaks Pressure Perturbation

6.3.1.1 Case A1: Two Peaks Pressure Perturbation (model with 33 core channels)

As explained in Section 6.1.1, several transient calculations have been performed with the RELAP5/PARCS coupled codes using the two different thermalhydraulic models.

In this first analysis, the reactor has been perturbed with a steam line pressure disturbance (see section 5.2.1 for the test description); the calculation has been carried out with the 33 channels T/H core nodalization.

The following three figures (figures 6.2, 6.3, 6.4) describe the transient behaviour of three thermalhydraulic parameters particularly significant in the instability analyses: core power, core inlet mass flow rate and steam line pressure.

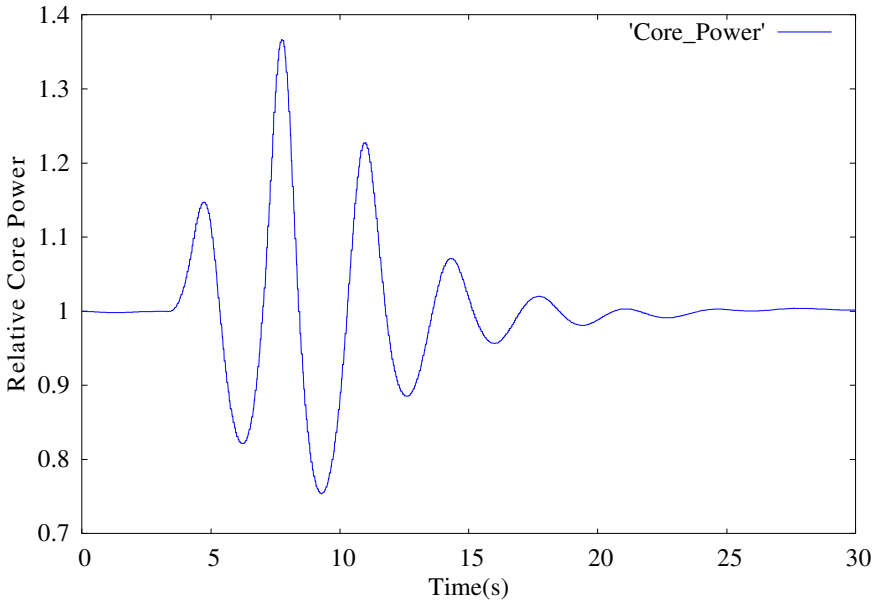

Figure 6-2: Relative core power variation during the transient for Case A1

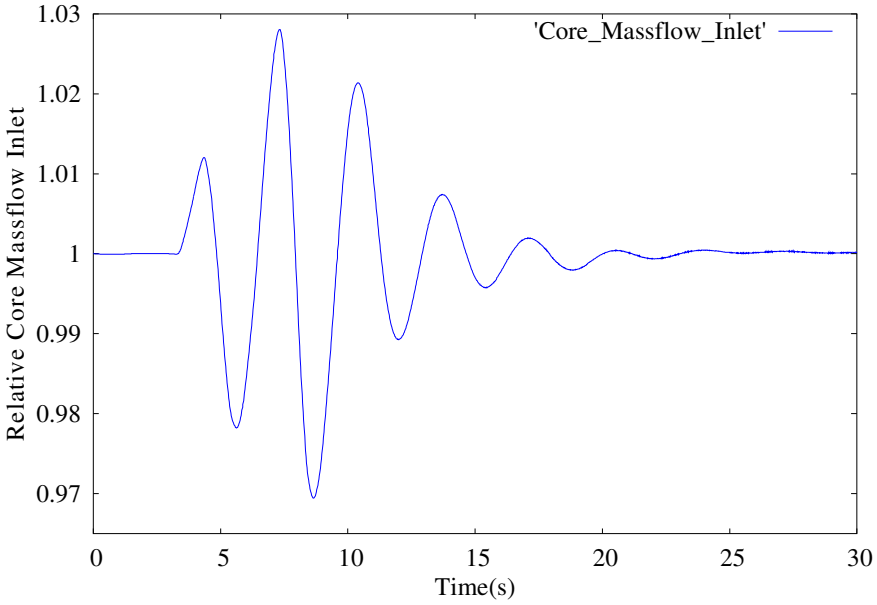

Figure 6-3: Relative core inlet mass flow rate variation during the transient for Case A1

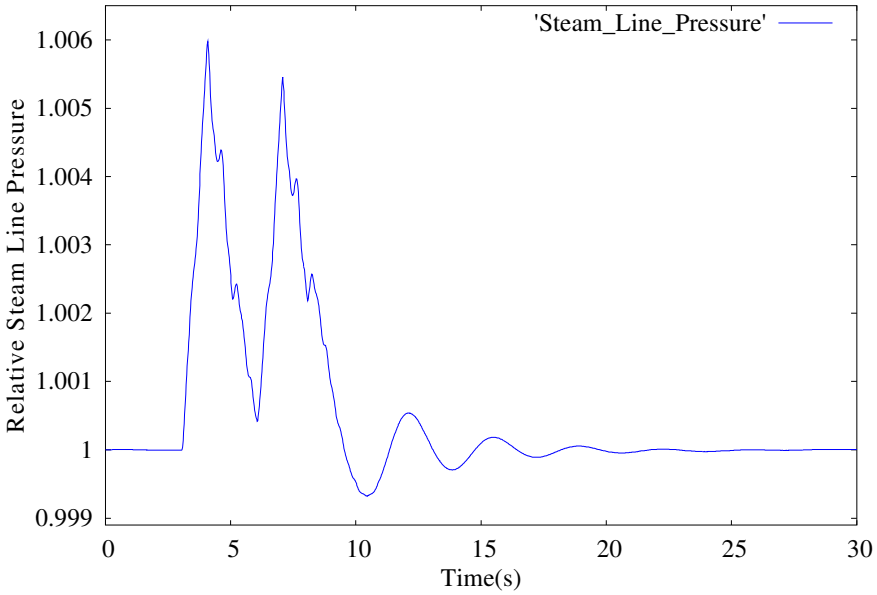

Figure 6-4: Relative steam line pressure variation during the transient for case A1

The disturbance in the steam line ends at 10 seconds and as it is clear from the figures the perturbation does not produce any unstable behaviour in the reactor: after the conclusion of the disturbance, the power oscillations decrease very rapidly, becoming negligible within few seconds.

With the nuclear cross-section provided by the transient calculation performed with RELAP5/PARCS, different analyses with the VALKIN code have been also carried out.

As explained in the Section 6.1.3, it is important to find a compromise between the number of modes and their updating time, in order to optimize the performance of the method. So, two transient calculations have been performed with VALKIN, with 1 and with 3 modes respectively, in order to analyze the influence of the number of modes in the results.

Figure 6.5 shows the power evolution obtained in the two analyses performed and the comparison with the one achieved with the RELAP5/PARCS calculation taken as reference[22]. It is possible to observe the good agreement

[22] The RELAP5/PARCS coupled codes has been taken as reference because are considered complete thermalhydraulic-neutronic codes.

among the results, even in the case in which a single mode was used; consequently, in order to reduce the CPU time but conserving the same accuracy, the analysis has been continued using only one mode.

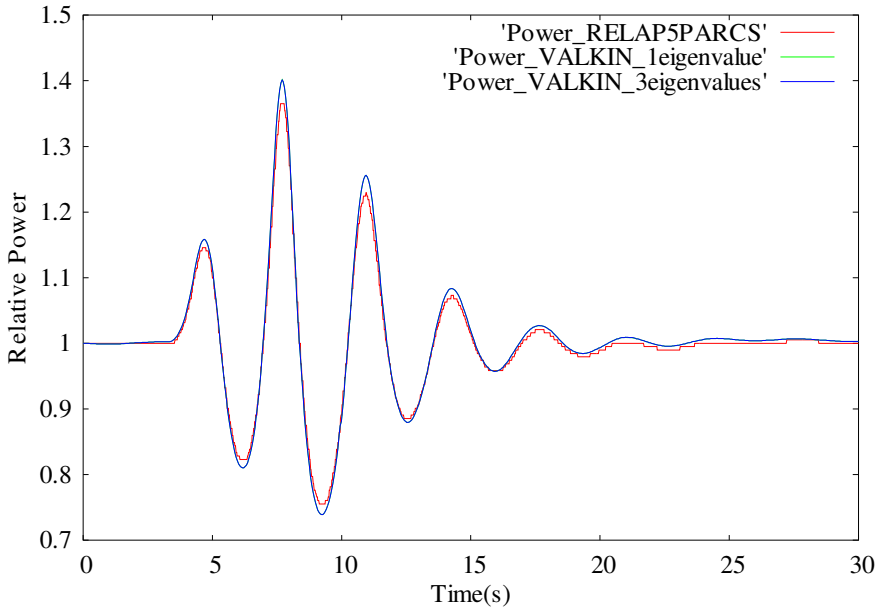

Figure 6-5: Comparison between the power evolution obtained with RELAP5/PARCS and the power evolution obtained using VALKIN code with different number of eigenvalues.

In figure 6.6 a detail of the power evolution is shown for the transient calculated using a single mode. The result obtained without updating the modes and updating the modes each 0.956 s and each 0.0956 s are compared with the reference one. It is possible to observe that the updating process increases the accuracy of the obtained solution.

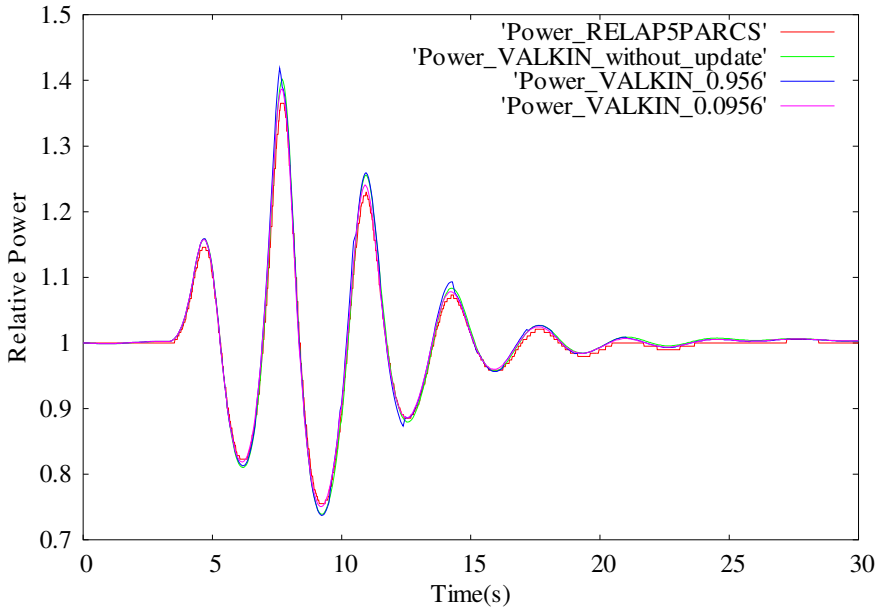

Figure 6-6: Comparison between the power evolution obtained with RELAP5/PARCS and the power evolution obtained using VALKIN code with 1 eigenvalue and different updating times.

The main difference in the transient appears in the maximum power peak achieved during the transient. As it was already mentioned, the relative error decreases as the updating time decreases.

To characterize the studied transients as in-phase or out-of-phase and also to study the importance of the amplitudes associated to the different modes during the transients, the time dependent modal amplitudes, $n_l(t)$, have been calculated for the fundamental mode and for two harmonics, using an updating time of 0.956 s.

Figure 6.7 shows the obtained evolutions of $n_0(t)$, $n_1(t)$ and $n_2(t)$.

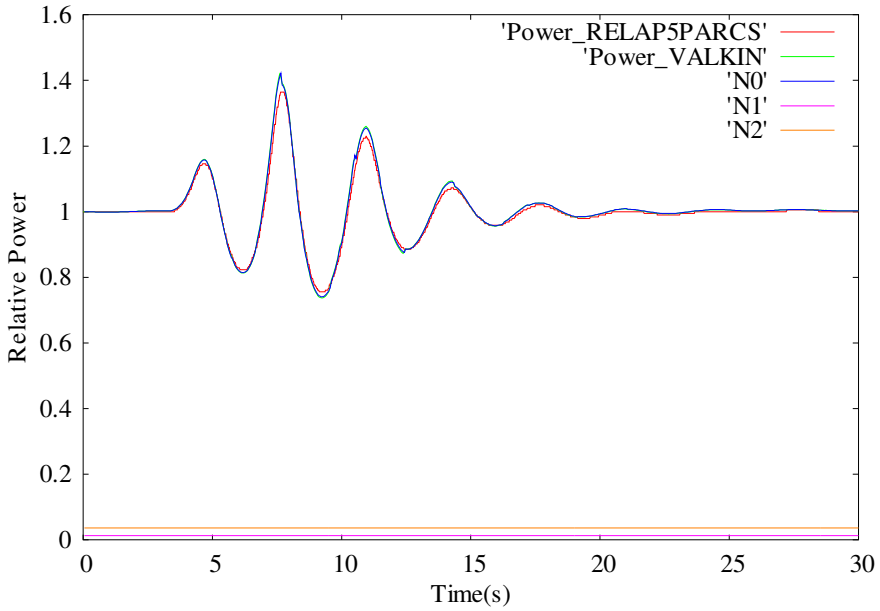

Figure 6-7: Power evolution with RELAP/PARCS and VALKIN, and amplitudes of the first three modes.

It is evident that the amplitude $n_0(t)$ is the dominant one during the oscillations, while $n_1(t)$ and $n_2(t)$ are nearly negligible; so, in this transient the reactor behaviour it is easily identifiable as in-phase.

Moreover, the above presented results for the power modal analyses have been complemented by considering the information provided by the simulation of the LPRM signals by RELAP5/PARCS. As explained in detail in Section 6.1.4, a modal decomposition of the neutronic power was performed from the local power distribution in the reactor core (made available by the coupled codes) and then, this decomposition was compared with the one achieved from the LPRM outputs also simulated by the same coupled codes.

In previous studies [25], it was shown that it is possible to consider for these analyses only the signals from one of the axial levels of LPRM's, consequently, the comparison has been carried out considering only the signals of the LPRM located at the axial Level B.

The results obtained for the amplitude evolutions associated with the fundamental mode ($a_0(t)$, plotted as N0_from_LPRM) and with two azimuthal

modes ($a_1(t)$, plotted as N1_from_LPRM and $a_2(t)$, plotted as N2_from_LPRM) are shown in figure 6.8.

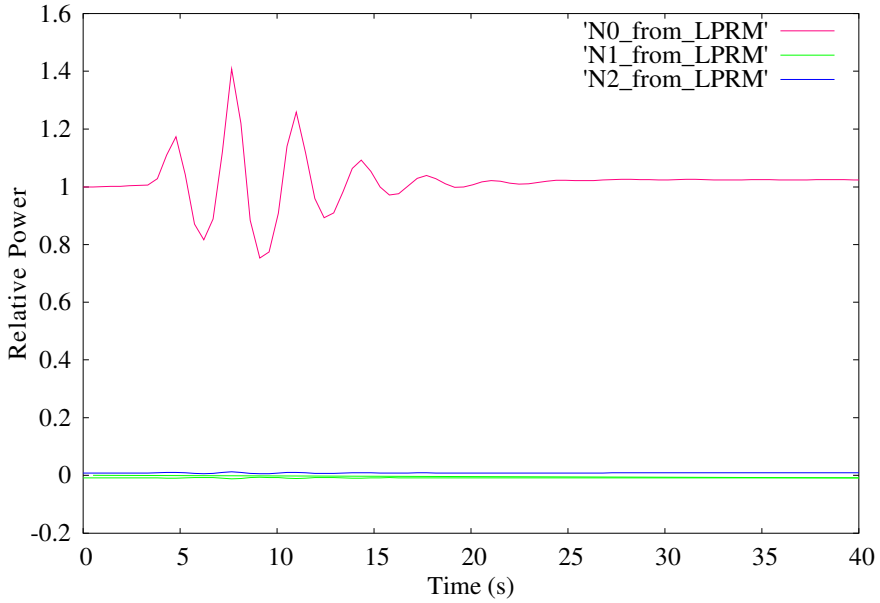

Figure 6-8: Amplitude evolutions obtained from the LPRM signals for case A1

The following figure represents the comparison among the fundamental amplitude achieved with the two different modal decompositions and the power evolution provided by the RELAP5/PARCS transient calculation.

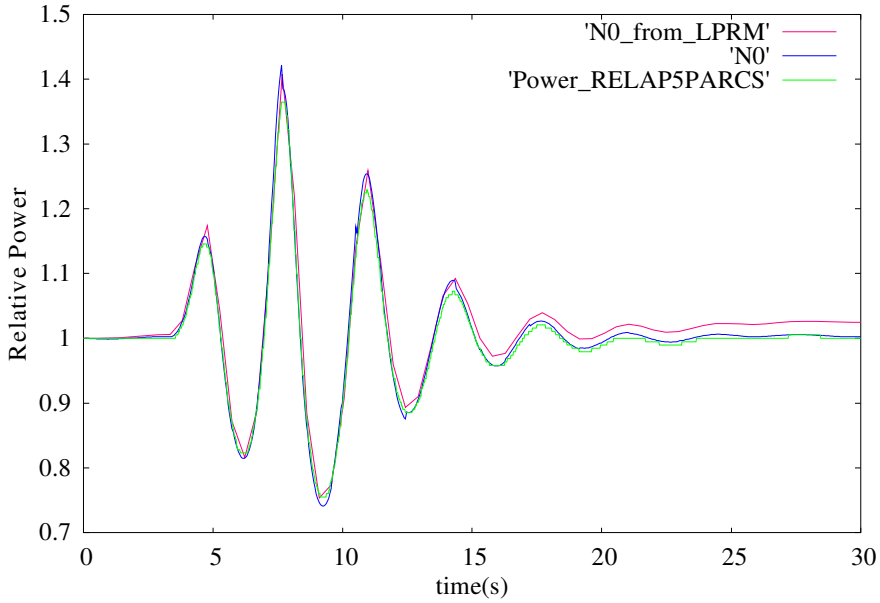

Figure 6-9: Comparison between the amplitudes obtained in the two distinct decompositions and the power evolution achieved with the RELAP5/PARCS calculation

The good agreement between the obtained results is clear: the maximum relative error it is about 0.027 % at the end of the transient.

Then, with a great saving of time, simply considering the signals from one of the axial level of LPRM's it is possible to achieve the same qualitative information as is obtained from the detailed nodal analysis in which it is necessary to know the power distribution for all the reactor nodes at each time step.

6.3.1.2 Case A2: Two Peaks Pressure Perturbation (model with 1 core channel)

With the RELAP5/PARCS coupled codes, the same test cases described in the previous section, i.e., a two peak steam line pressure disturbance were performed adopting the core model with a single channel.

In order to show the reactor evolution during the tests, the following figures report the trends of core power, core mass flow inlet rate and steam line pressure.

As it can be noted from the figures, the system has a stable behaviour: after the end of the perturbation the oscillations are damped and the reactor tends to a steady state as the time simulation time advance.

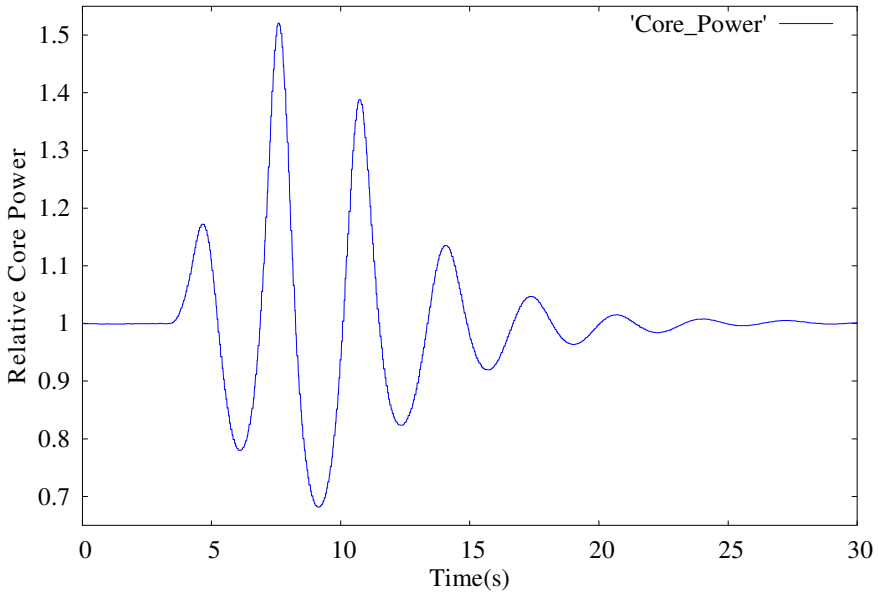

Figure 6-10: Relative core power variation during the transient for case A2

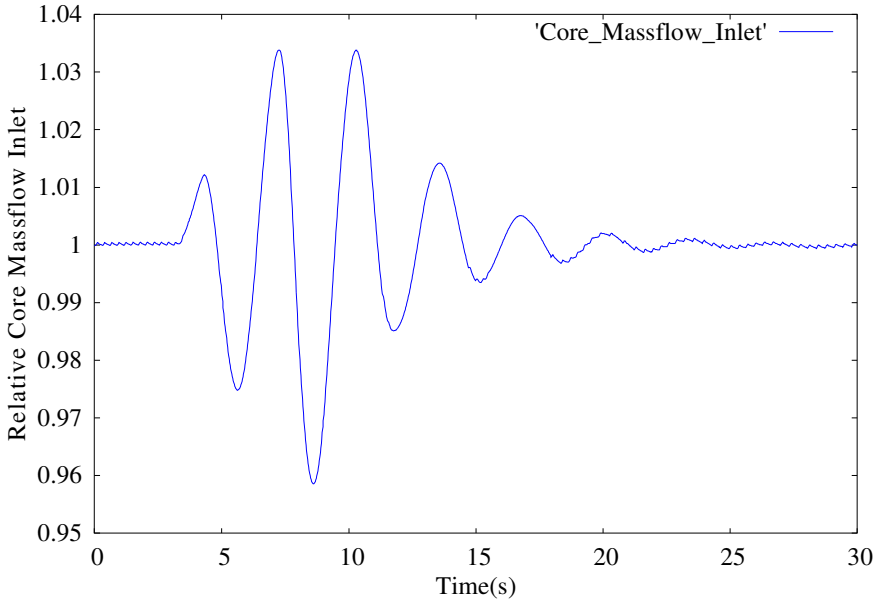

Figure 6-11: Relative core inlet mass flow rate variation during the transient for case A2

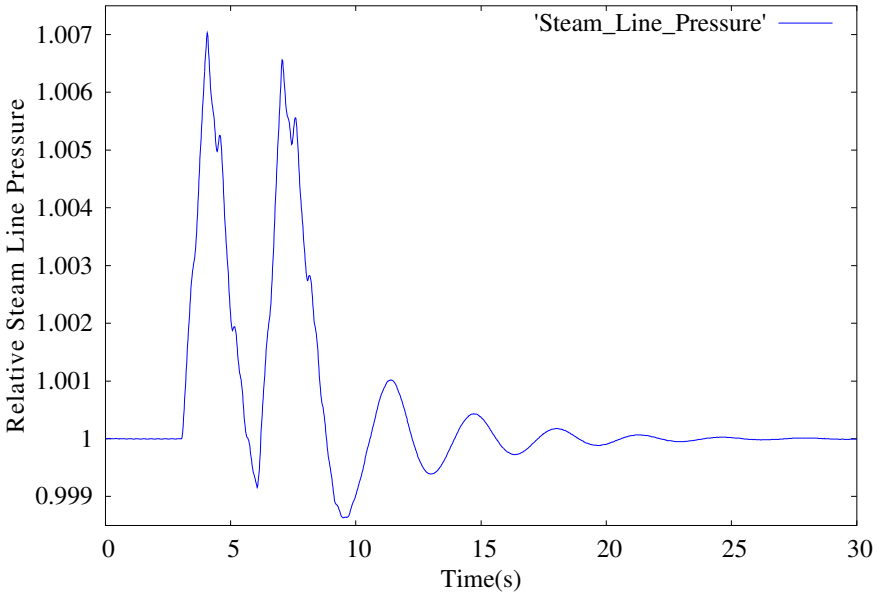

Figure 6-12: Relative steam line pressure variation during the transient for case A2

Also in this case, an analysis with the VALKIN code was performed with the nuclear cross-section provided by the RELAP5/PARCS calculation; all the tests have been run using only one mode.

In figure 6.13 and 6.14 details of the power transient history are shown; the solutions obtained without updating the modes and updating the modes each 0.956 s are compared with the solution taken as reference.

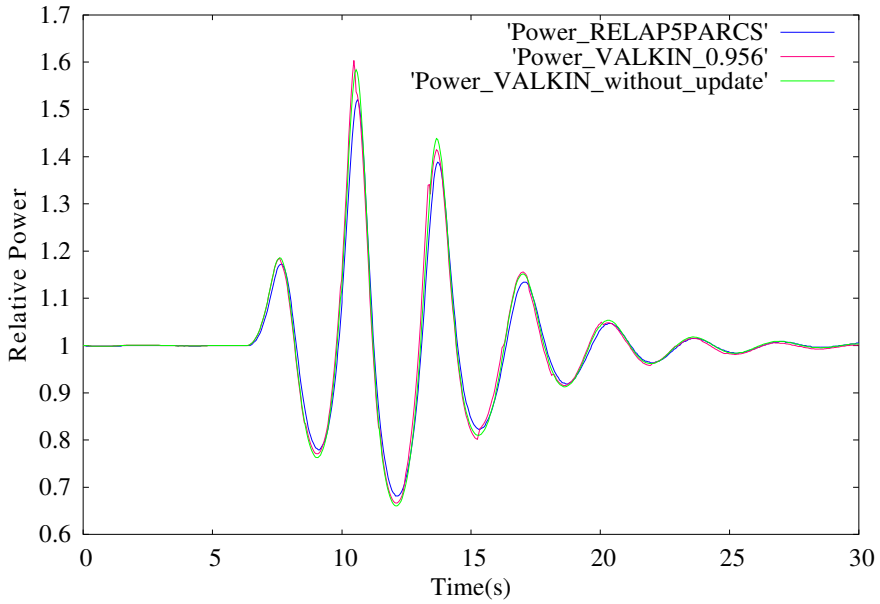

Figure 6-13: Comparison between the power evolution obtained with RELAP5/PARCS and the power evolution obtained using VALKIN code with 1 eigenvalue and different updating times.

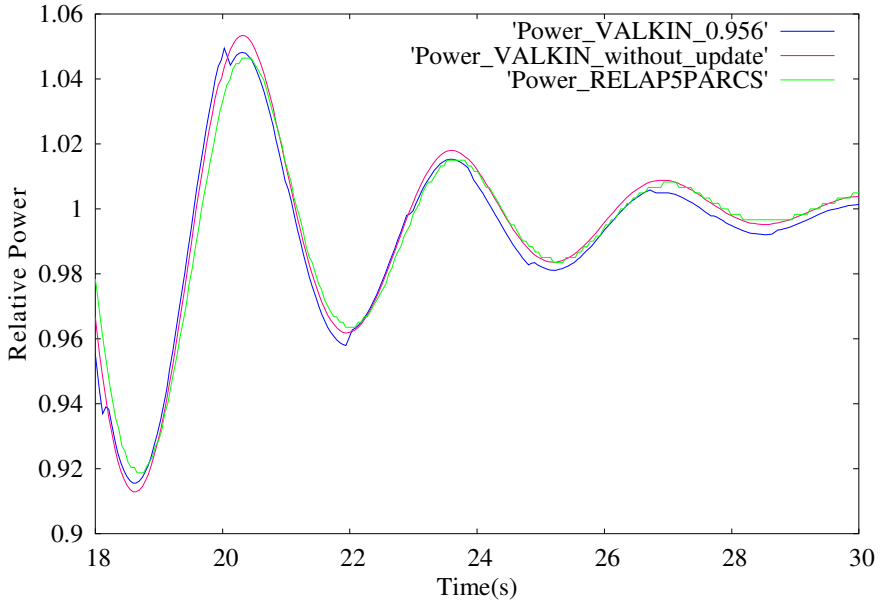

Figure 6-14: Particular of the power evolution comparison plotted in the figure 6.13

The good agreement among the results calculated with both codes is evident in the previous figures 6.13 and 6.14. It is also noticeable as the updating

process improves the solution especially concerning the maximum and minimum of the oscillation.

6.3.1.3 Case A: Two Peaks Pressure Perturbation (comparison between the results achieved with the two different nodalizations)

In the next figures (figures 6.15, 6.16, 6.17) comparison between the calculated trends obtained with the two different thermalhydraulic models are shown:

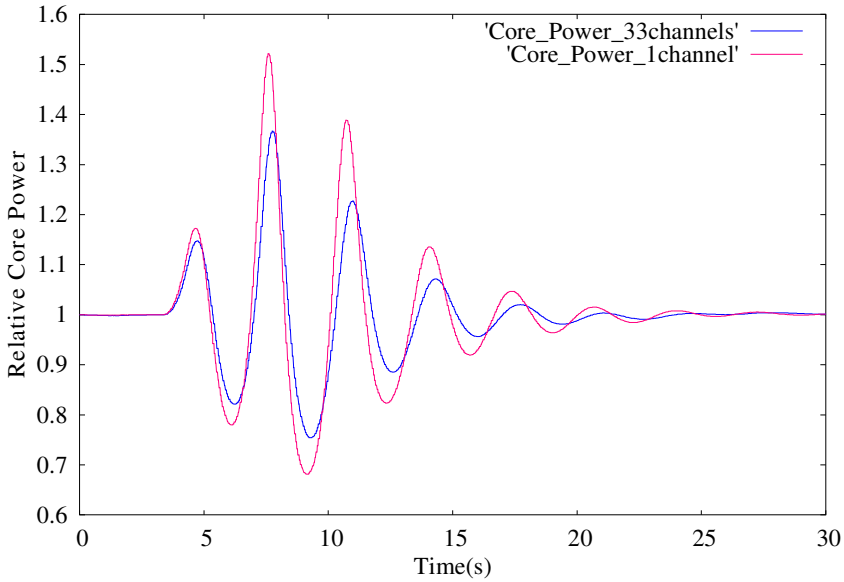

Figure 6-15: Comparison between the relative core power trends obtained with the two different models

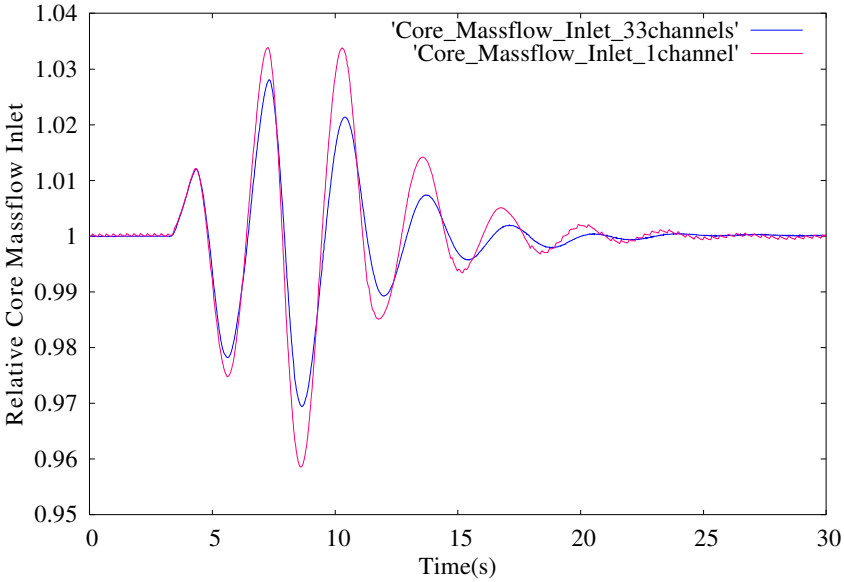

Figure 6-16: Comparison between the relative core inlet mass flow rate transient evolutions obtained with the two different models

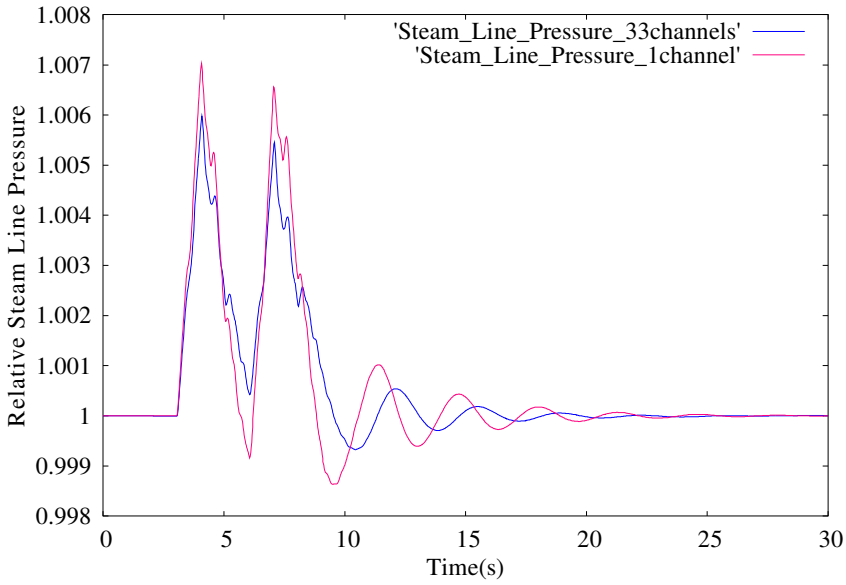

Figure 6-17 Comparison between the relative steam line pressure histories during the transient obtained with the two different models

The figures show that the results obtained using the two different core nodalizations are similar; however, it is evident that in the test performed with a single T/H channel the oscillatory trend lasts for a longer time, i.e., the reactor seems to be slightly less stable in this case. Moreover, it is also remarkable that the oscillations generated in the case of a single channel are anticipated in phase with respect to the oscillations developed in the other simulation.

6.3.2 Case B: Pseudo Random Sequence Pressure Perturbation

6.3.2.1 Case B1: Pseudo Random Sequence Pressure Perturbation (model with 33 core channels)

In this section the results of a RELAP5/PARCS transient calculation are discussed where the reactor is disturbed with a perturbation in the steam line consisting of fifty pressure peaks obtained with a random function (see section 6.1.2); the calculation has been performed adopting the model with 33 thermalhydraulic channels for the core.

In order to represent the system evolution during the transient, in the figures 6.18, 6.19, 6.20 the simulated core power, core inlet mass flow rate and steam line pressure trend are shown.

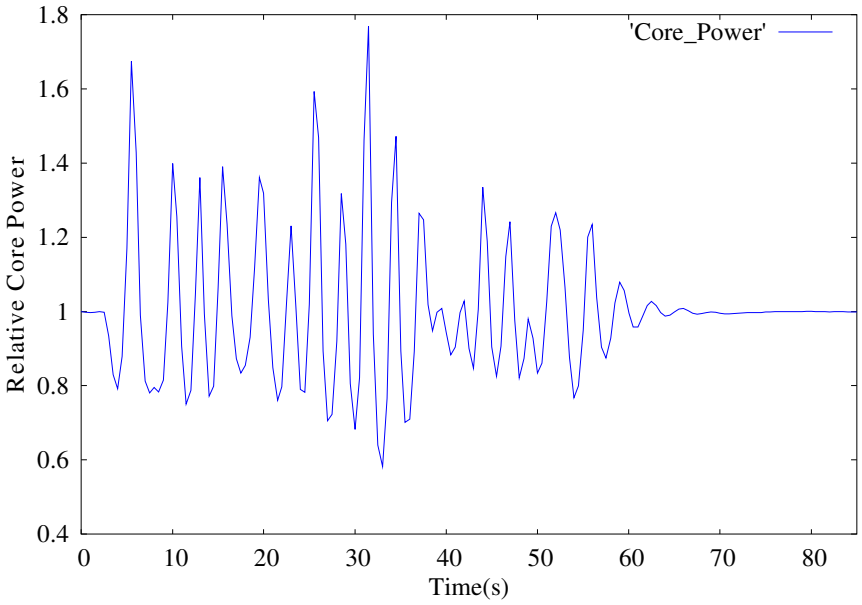

Figure 6-18: Relative core power evolution during the transient for case B1

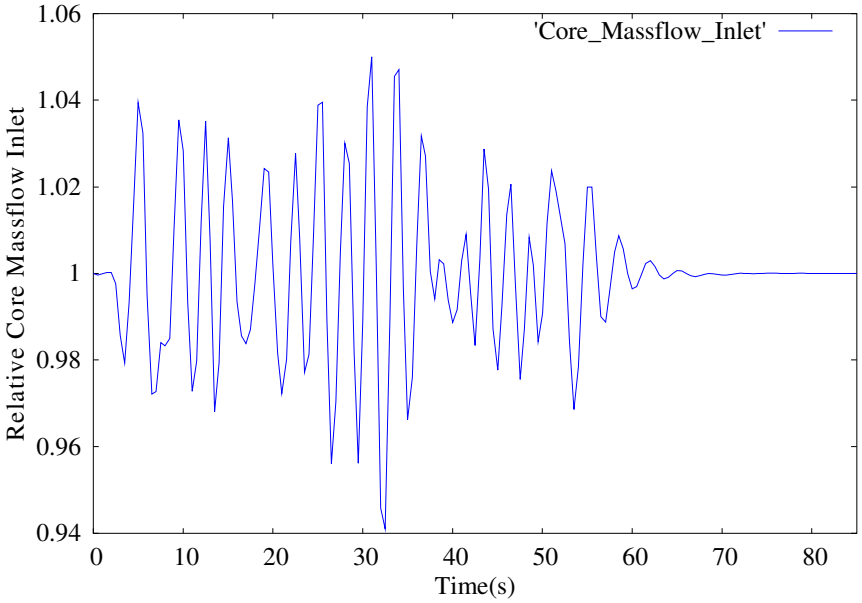

Figure 6-19: Relative core inlet mass flow rate evolution during the transient for case B1

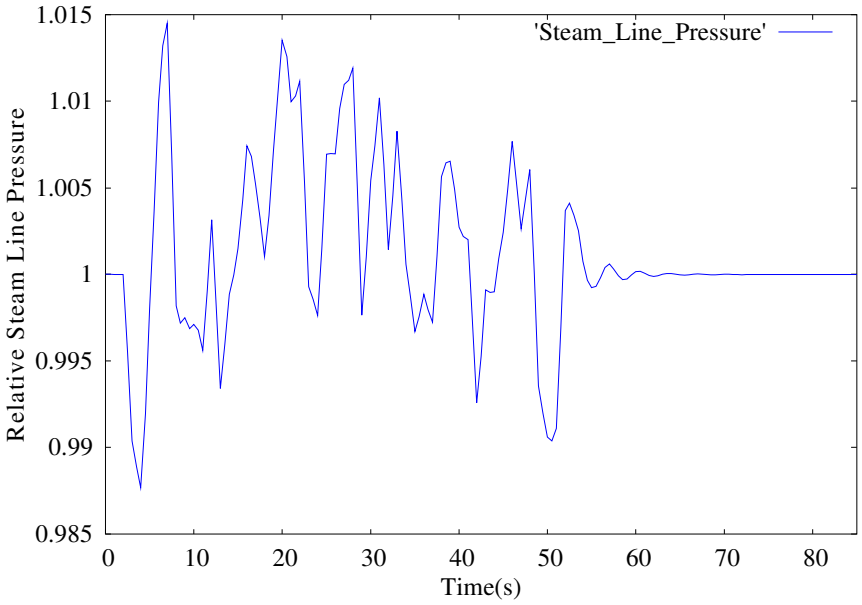

Figure 6-20: Relative steam line pressure evolution during the transient for case B1

Observing the figures, it is clear that the perturbation does not produce any long term effect in the state of the system: the oscillation originated owing to the disturbance dies out in approximately 8 s after the end of the perturbation and then the reactor goes back to the initial condition.

With the nuclear cross-section obtained in the RELAP5/PARCS transient calculation an analysis with the VALKIN code has been then carried out.

As the reactor behaviour is nearly stable, it is sufficient to use only one mode and to perform only two tests: without updating the process and updating the process each 0.9766 s.

In the next figures (figures 6.21, 6.22) the power transient histories simulated with the VALKIN codes are compared with the solution provided by the RELAP5/PARCS calculation.

The good agreement among the results calculated with both codes it is evident in the figures and, as it was expected, the solution improves using the updating procedure.

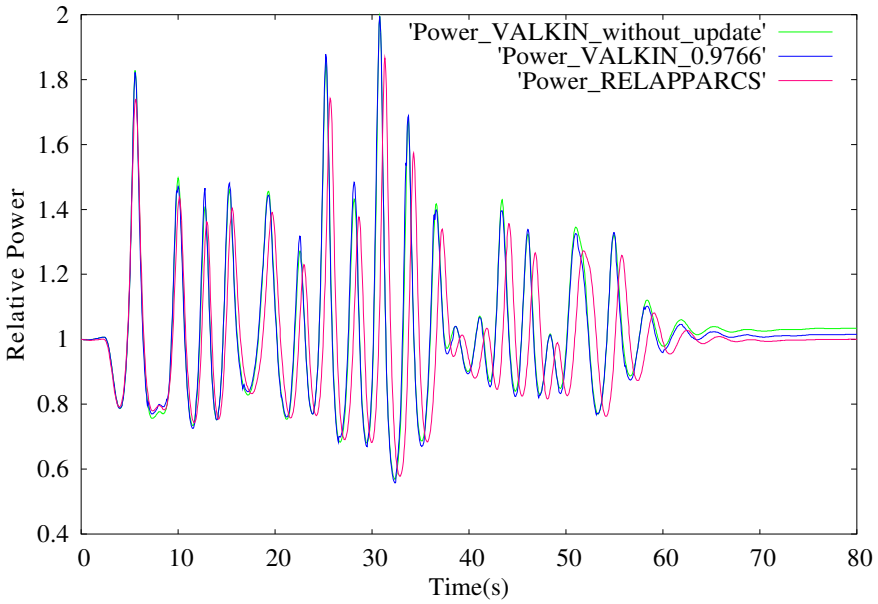

Figure 6-21: Comparison between the power evolution obtained with RELAP5/PARCS and the power evolution obtained using VALKIN code with 1 eigenvalue and different updating times.

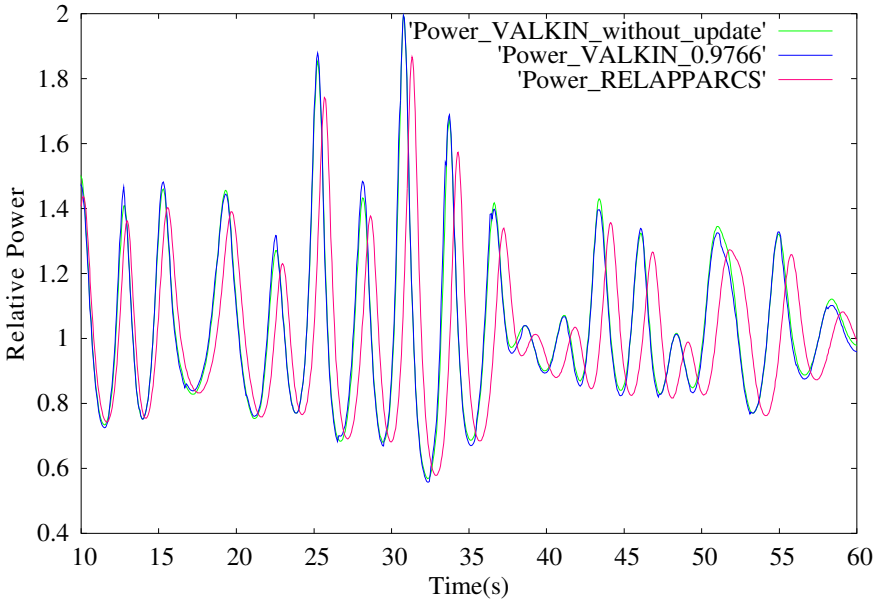

Figure 6-22: Particular of the comparison plotted in figure 6.21: transient evolution between 10 sec and 60 sec

6.3.2.2 Case B2: Pseudo Random Sequence Pressure Perturbation (model with 1 core channel)

The same perturbation used in case B1 (see section 6.3.2.1) has been applied to trigger oscillations in the system in this RELAP5/PARCS transient calculation that adopts the single channel TH model of the core.

In the figures 6.23, 6.24 and 6.25 the power, the core inlet mass flow rate and the steam line pressure evolution during the entire transient are represented respectively.

As it can be noted, the system also in this case does not develop an unstable behaviour, in fact, the oscillations after the conclusion of the disturbance (at 53s), decrease very rapidly, becoming negligible after few seconds.

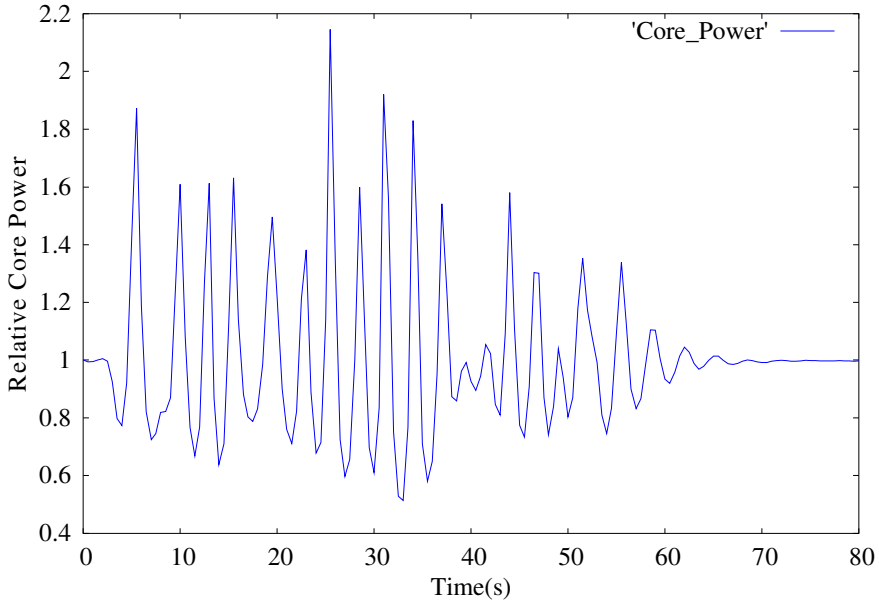

Figure 6-23: Relative core power trend during the transient for case B2

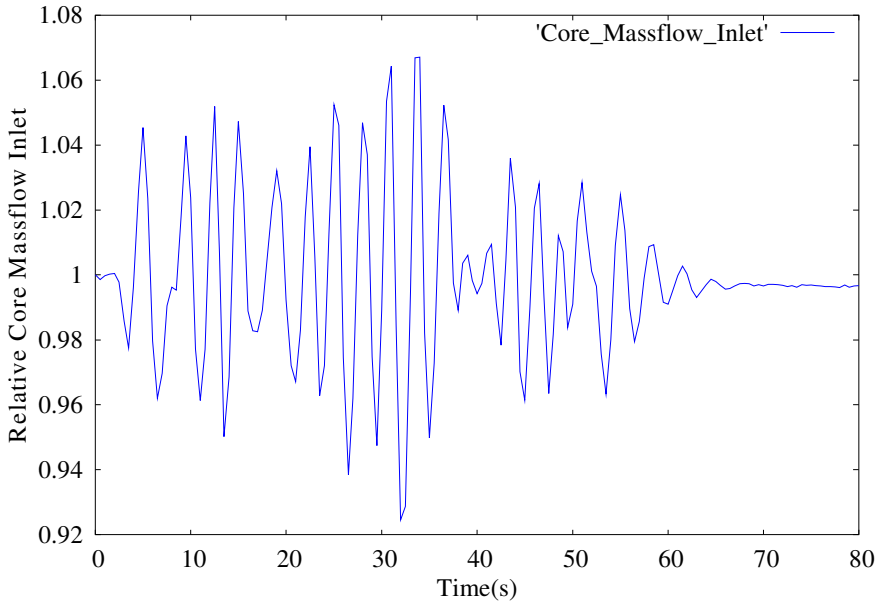

Figure 6-24: Relative core inlet mass flow rate trend during the transient for case B2

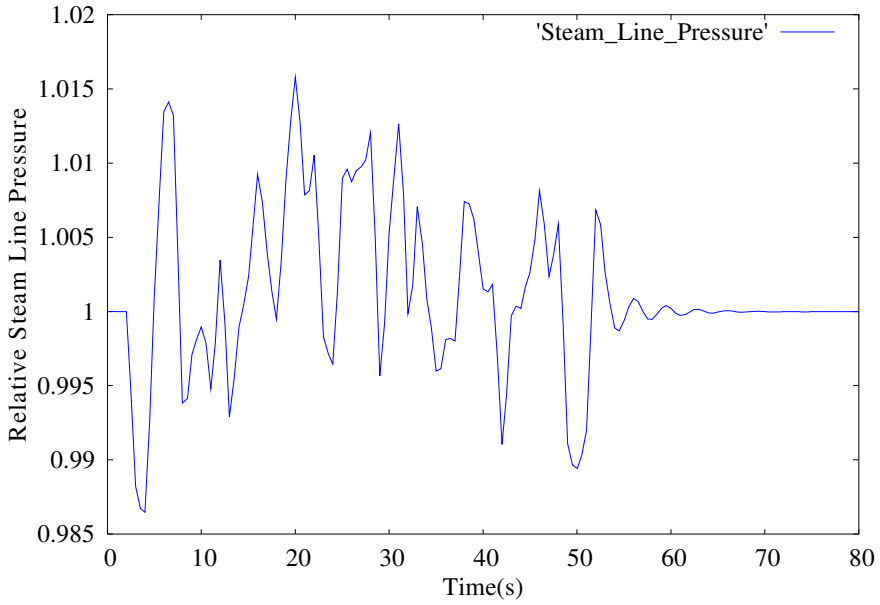

Figure 6-25: Relative steam line pressure trend during the transient for case B2

Additionally, analyses with the VALKIN codes have been carried out using the nuclear cross-section provided by the RELAP5/PARCS transient calculation.

In similarity with what found in the previous case, only two tests were performed, both of them adopting only a single mode, without and with updating.

In the figures 6.26, 6.27 and 6.28 details of the power transient evolution obtained by the analysis are shown.

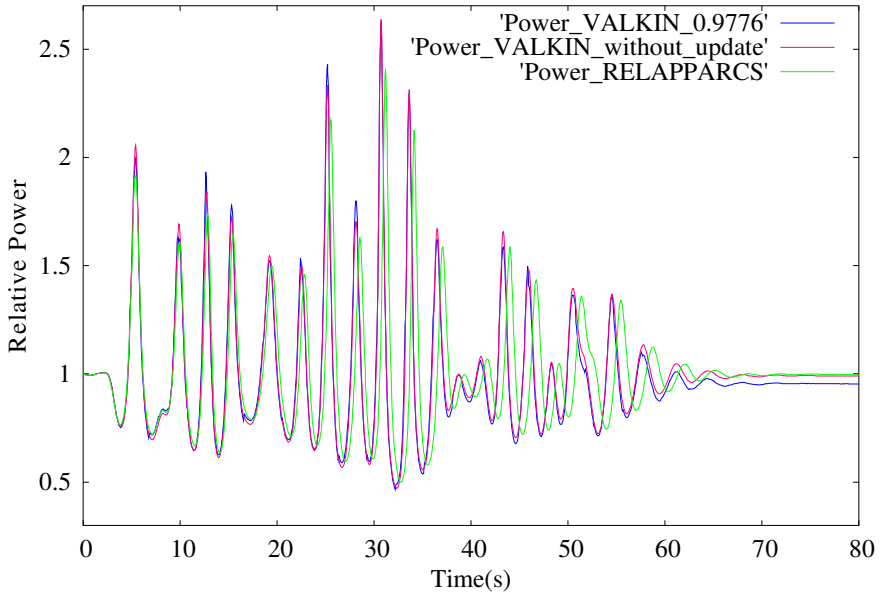

Figure 6-26: Comparison between the power evolution obtained with RELAP5/PARCS and the power evolution obtained using VALKIN code with 1 eigenvalue and different updating times.

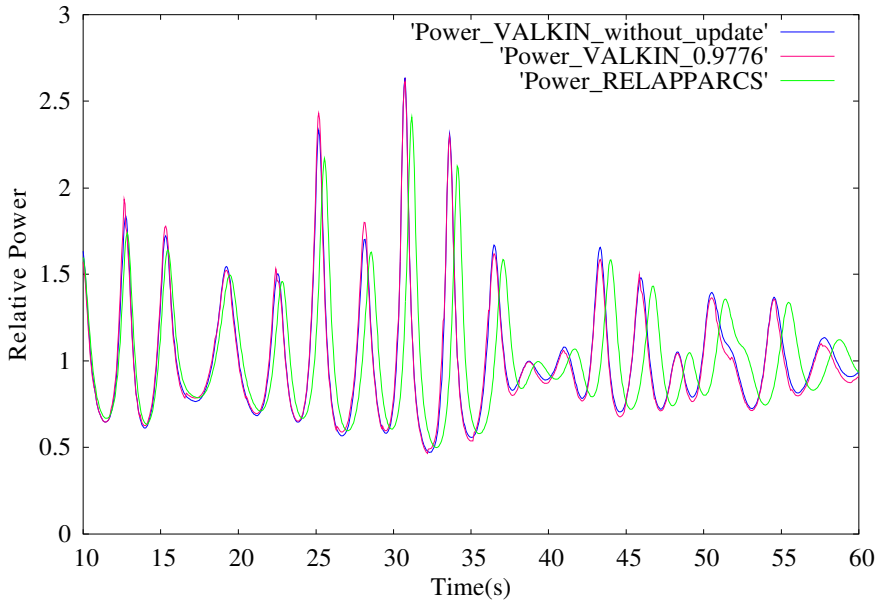

Figure 6-27: Particular of the comparison plotted in figure 6.26: transient evolution from 10s to 60 s

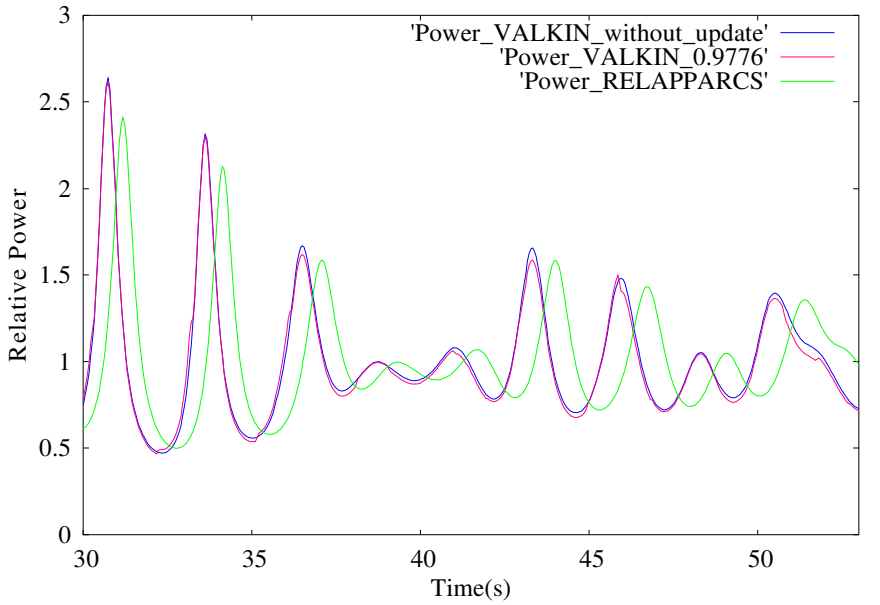

Figure 6-28: Particular of the comparison plotted in figure 6.26: transient evolution from 30s to 53s

Also in this case, satisfactory results are achieved with the VALKIN calculations: there is a good agreement between the solutions provided by the code and RELAP5/PARCS. It is noticeable that, as in the previous cases, the updating process improves the results, especially in the maxima and minima of the oscillations (see figure 6.28); considering the figures it is also possible to observe that in similarity with case B1, the VALKIN solutions initially oscillate

with the same frequency as in the reference RELAP5/PARCS calculation, though the frequency decreases later on..

This slightly phase-displacement can explained noting that the coupled codes RELAP5/PARCS use a variable time step, whereas for the VALKIN code the time step is imposed in the input.

6.3.2.3 Case B: Pseudo Random Sequence Pressure Perturbation (comparison between the results achieved with the two different nodalizations)

The next figures compare the core power, the core inlet mass flow rate and the steam line pressure evolutions simulated for case B with the two different core T/H models.

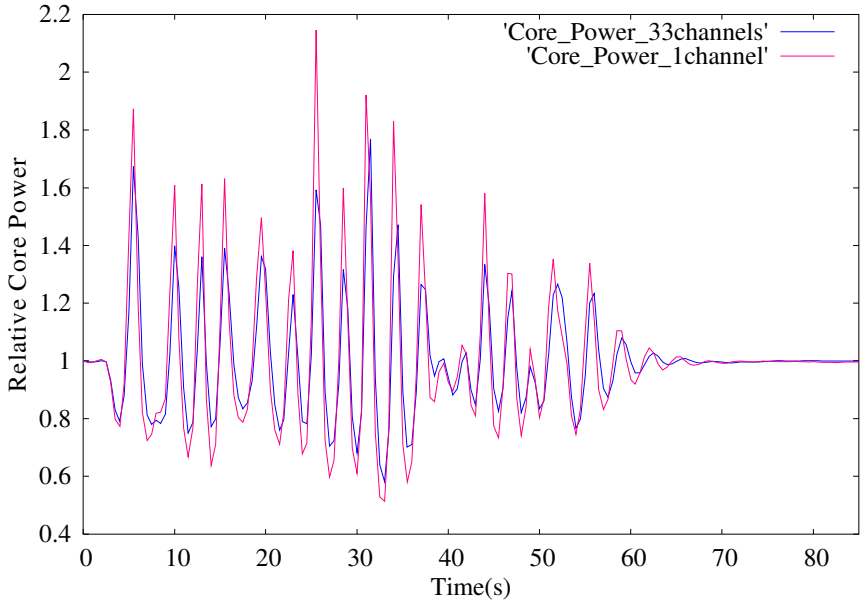

Figure 6-29: Comparison between the relative core power trends obtained with the two different models

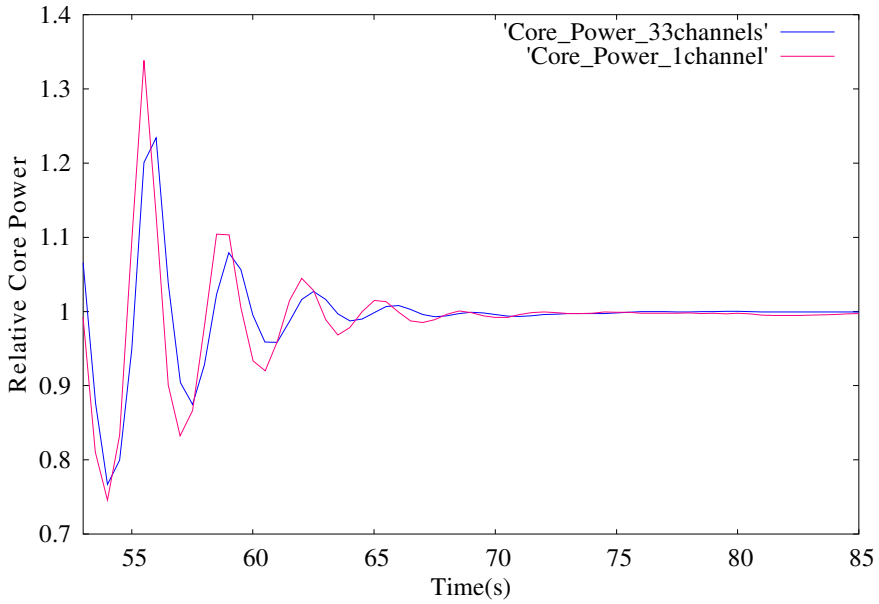

Figure 6-30: Particular of the core power trends comparison plotted in the preceding figure: power histories from the end of the perturbations to the end of the transient

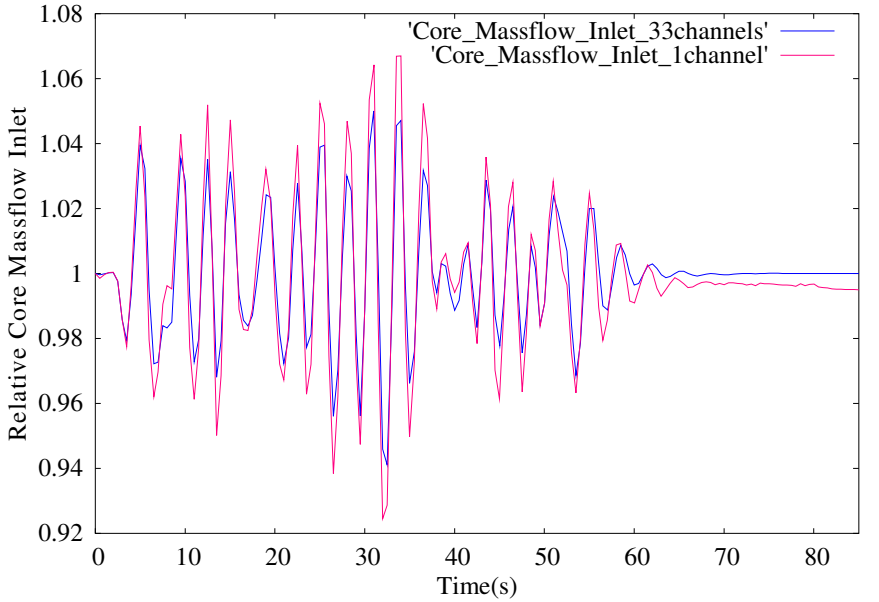

Figure 6-31: Comparison between the relative core inlet mass flow rate transient evolutions obtained with the two different models

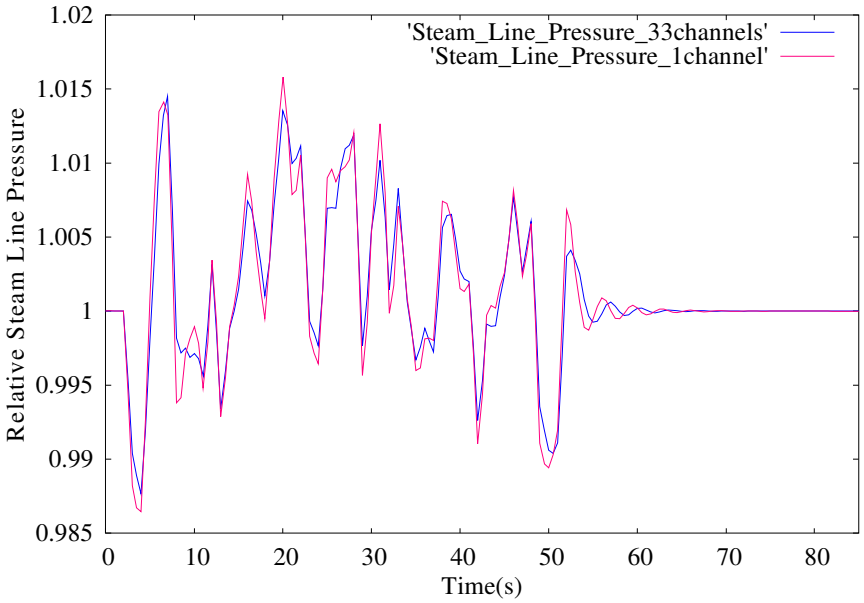

Figure 6-32: Comparison between the relative steam line pressure histories during the transient obtained with the two different models

Considering the figures the very good agreement between the results achieved with the two different thermalhydraulic modelling appears. The observed differences are similar to those obtained for case A; in particular, with the 33 channels T/H core model the system appears more stable that with the single channel nodalization and a slight phase shift among the two trends is observed (see figure 6.30).

6.3.3 Case C: Two Peaks Pressure Perturbation with a modified axial power distribution

6.3.3.1 Case C1: Two Peaks Pressure Perturbations with a modified axial power distribution (model with 33 core channels)

With the RELAP5/PARCS coupled codes a transient starting with control rod movement was performed, in the aim to modify the axial power distribution (the control rod movement is described in section 5.2.3). For this analysis the 33 T/H channels core model has been used.

In figure 6.33 the change in the reactor axial power shape after the control rod movement is shown.

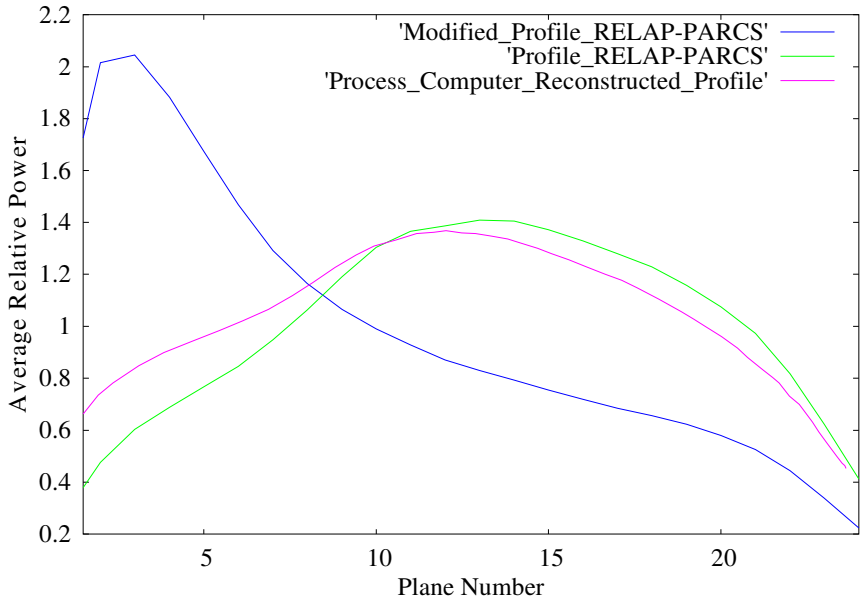

Figure 6-33: Comparison between the axial power distributions calculated before and after the control rod movement in case C1 and the reference one

The variation of the axial power profile, that assumes a bottom peaked shape, produces in the system an unstable behaviour; after the end of the control rod movement (at 8s), self-sustaining oscillations with a frequency of about 0.5 Hz are observed. In the following figures, the details of this oscillating trend are reported for core power, core inlet flow rate and steam line pressure

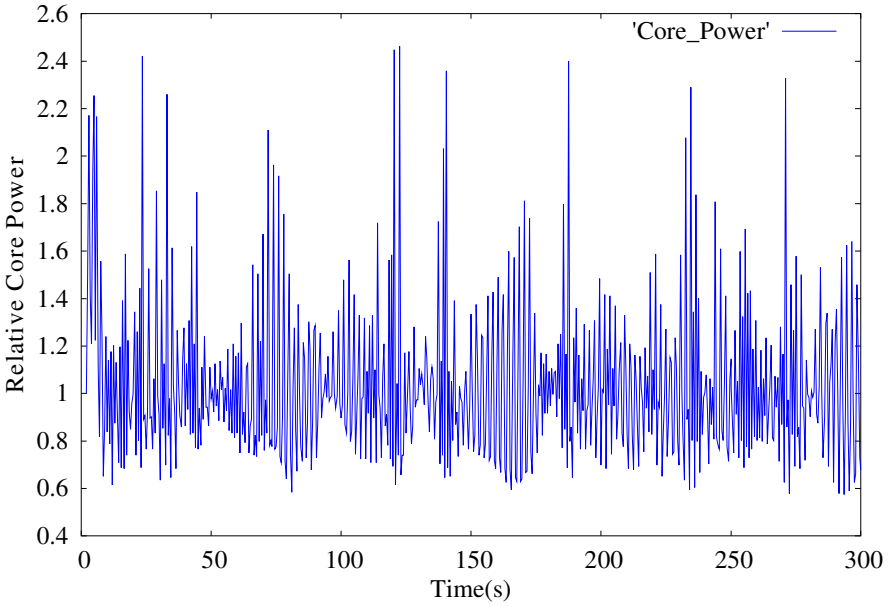

Figure 6-34: Reactor core power in case C1

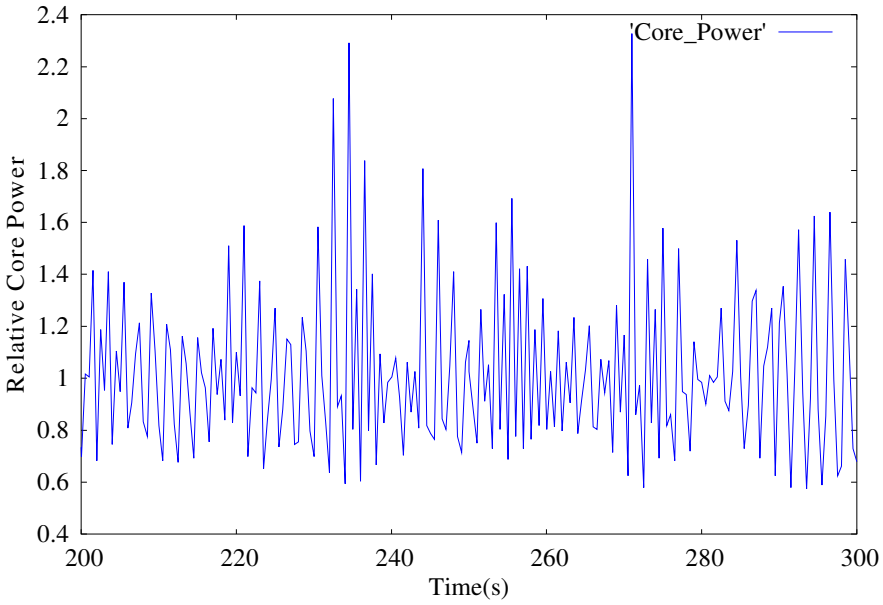

Figure 6-35: Particular of the power oscillation in case C1

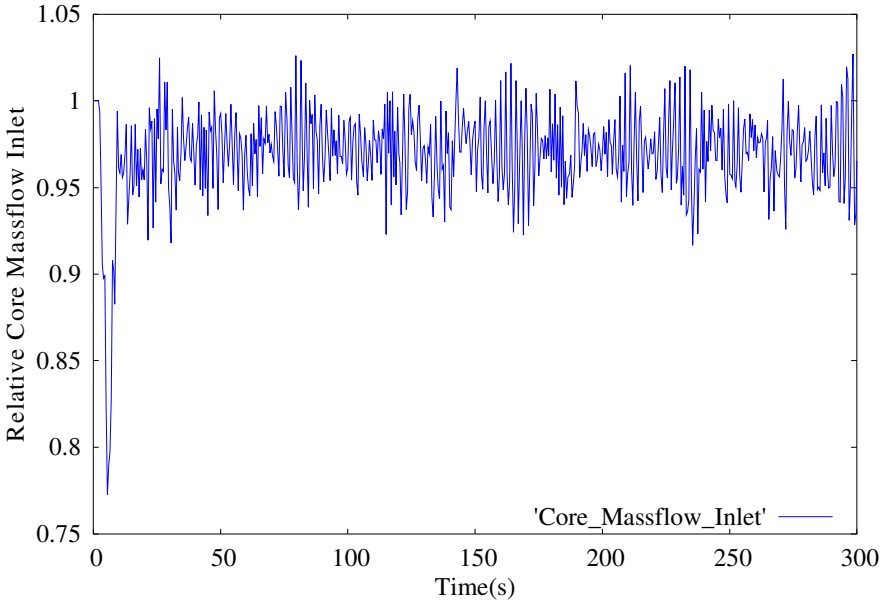

Figure 6-36: Core inlet mass flow rate in case C1

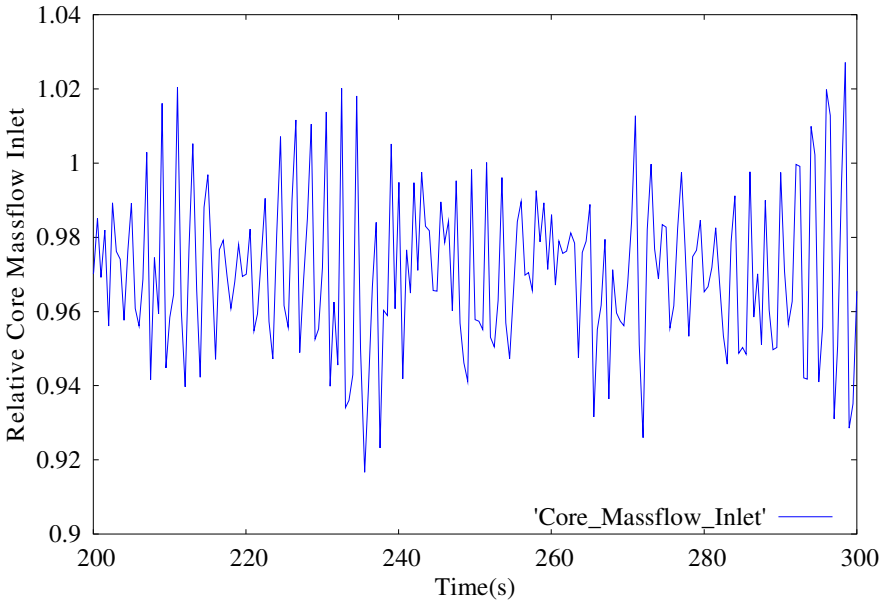

Figure 6-37: Particular of the core inlet flow rate oscillation in case C1

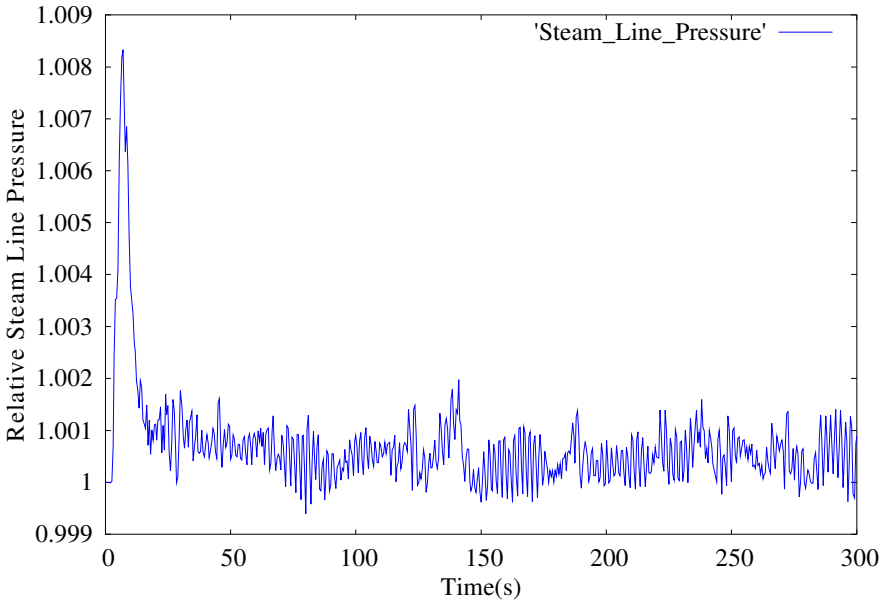

Figure 6-38: Steam line pressure in case C1

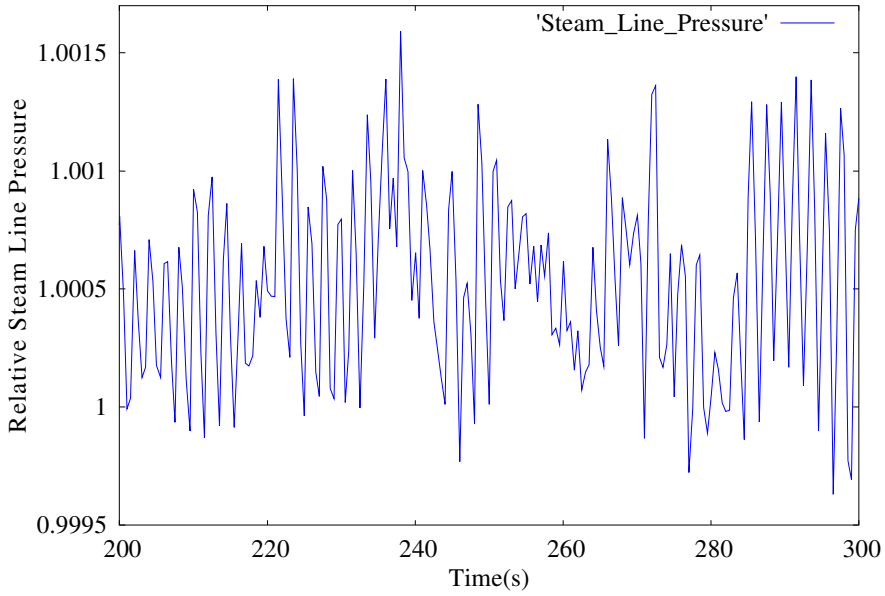

Figure 6-39: Particular of the steam line pressure oscillation in case C1

From the figures it is possible to see that, after control rod movement, the amplitude of the oscillations remains statistically constant in time, though a rather chaotic pattern appears.

After 300 s from transient start the oscillation behaviour continues to be regular; so, the reactor was perturbed again with a two peak steam line pressure perturbation (similar to the one in case A) in order to analyze the effect of a further disturbance on the unstable behaviour.

The perturbation begins at 307 s and ends at 312 s; as it is clear from the following figures, the disturbance does not produce any consequence on the reactor parameters trends, that immediately return to the initial oscillation conditions.

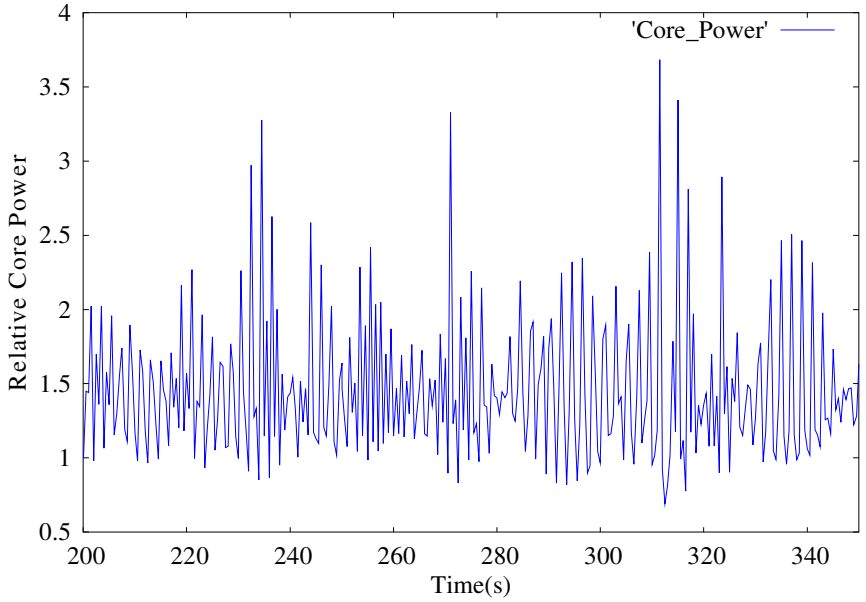

Figure 6-40: Particular of the reactor core power history during the transient in case C1

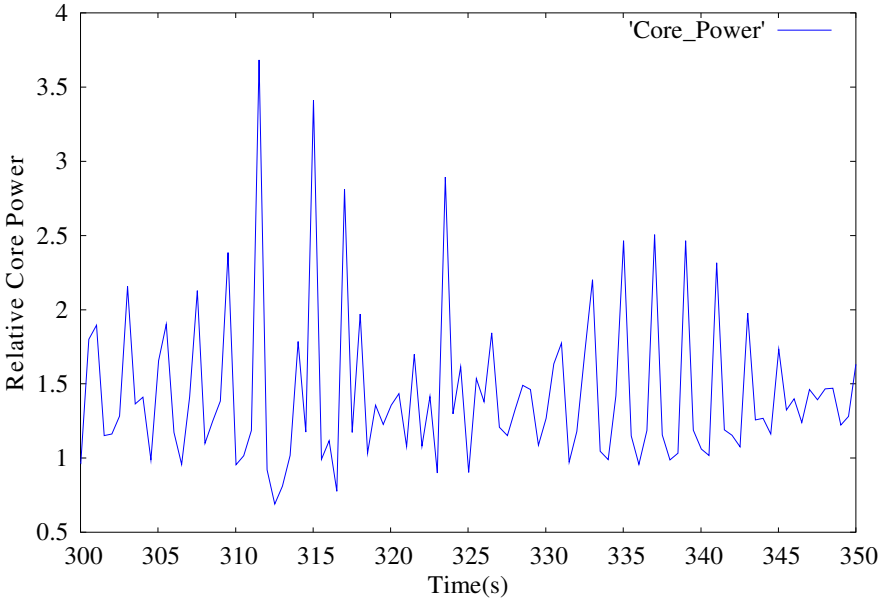

Figure 6-41: Reactor core power trend during the perturbation in case C1

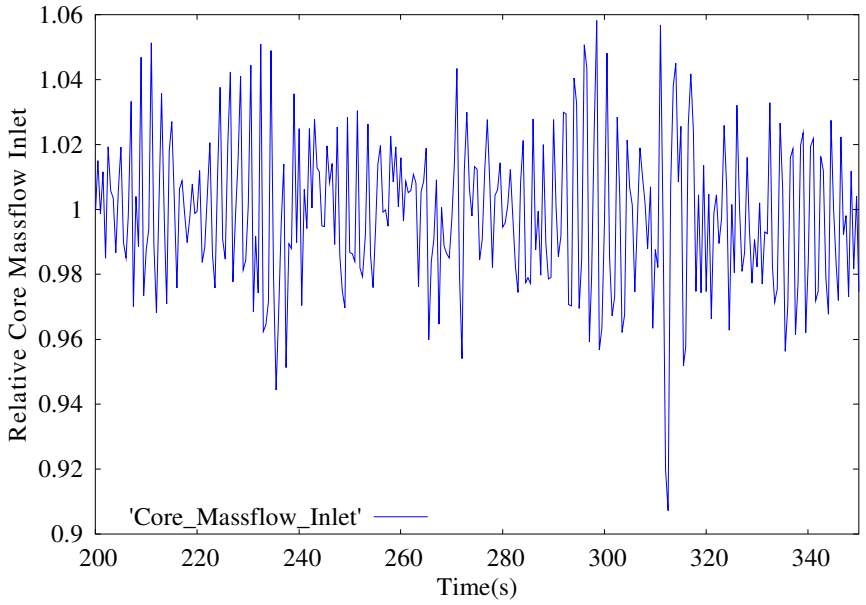

Figure 6-42: Particular of the reactor core inlet mass flow rate history during the transient in case C1

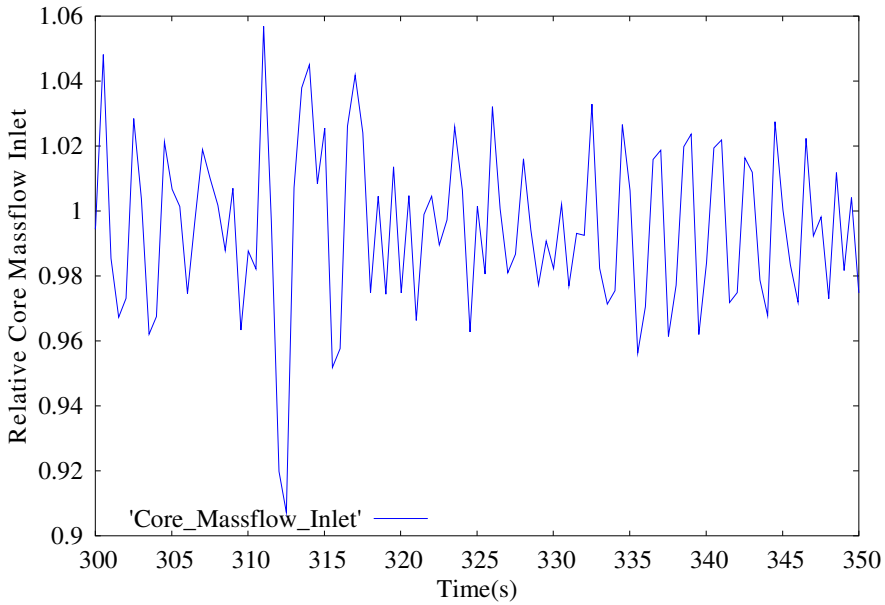

Figure 6-43: Reactor core inlet mass flow rate trend during the perturbation in case C1

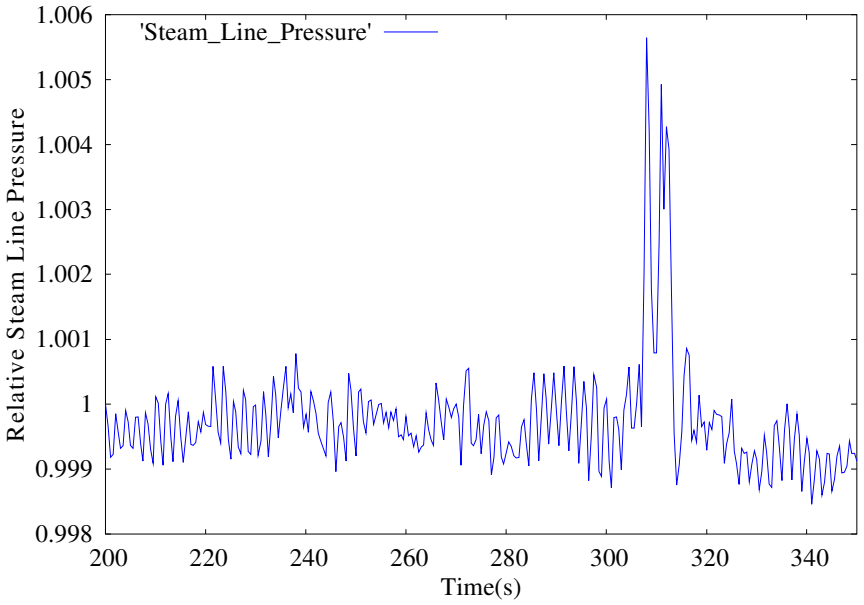

Figure 6-44: Particular of the steam line pressure history during the transient in case C1

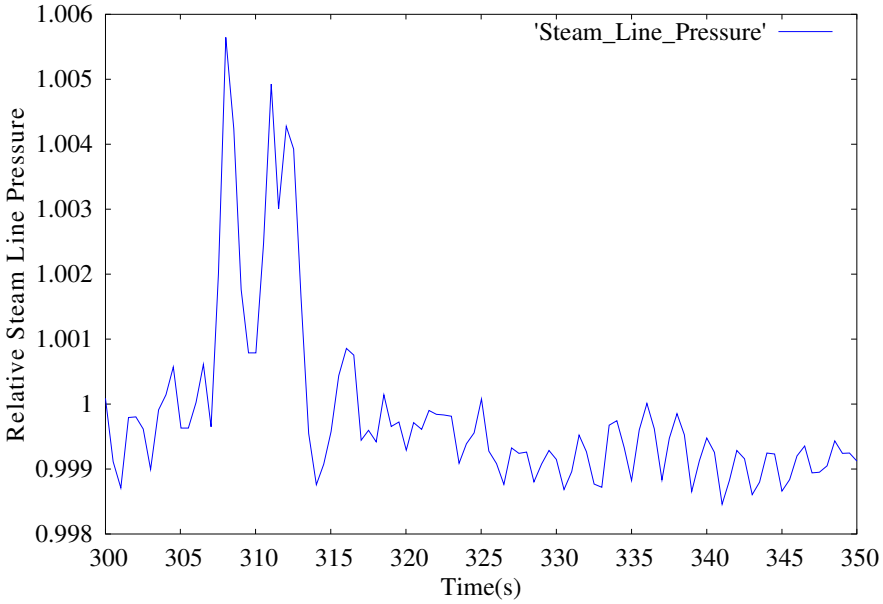

Figure 6-45: Steam line pressure during the perturbation in case C1

With the aim to make a more careful analysis of the instability recognized in the RELAP5/PARCS simulation, using the nuclear cross-sections provided by the transient calculation performed with the coupled codes, a number of analyses with the VALKIN code has also been carried out.

Figure 6.46 shows the power evolution for the transients calculated using 1 mode: it has been compared the results obtained without updating the mode and updating the mode each time step (i.e. each 0.0499 seconds) with the reference one (RELAP5/PARCS solution).

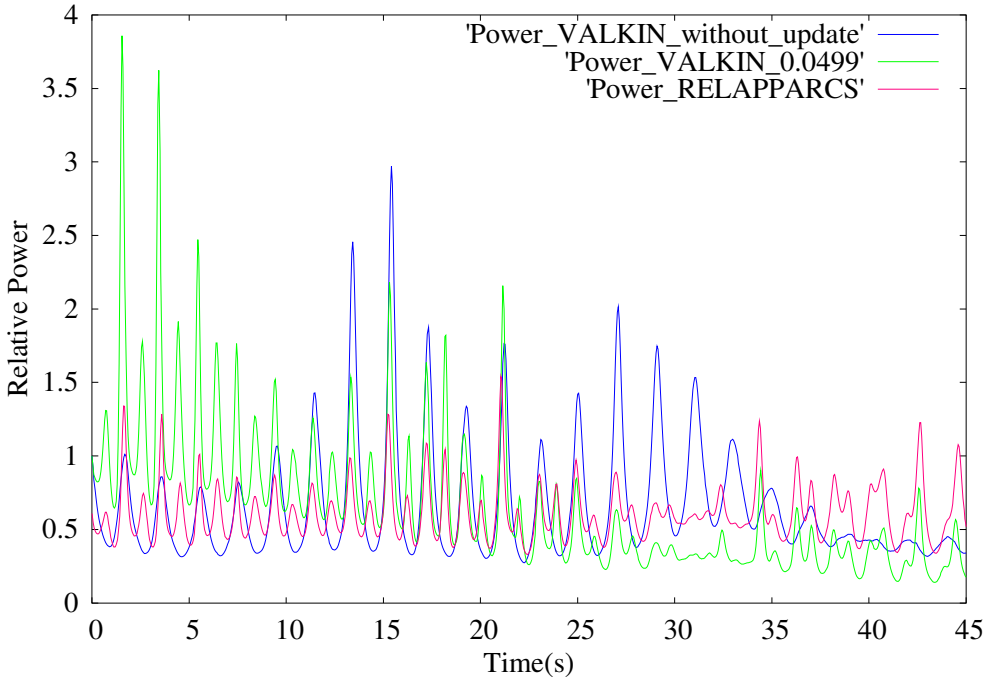

Figure 6-46: : Comparison between the power evolution obtained with RELAP5/PARCS and the power evolution obtained using VALKIN code with 1 eigenvalue and different updating times.

It is clear from the figure 6.46 that update in this case is absolutely necessary: the cross-sections change strongly from a time step to the next one and these relevant spatial changes make indispensable an updating of the spatial solution to obtain meaningful result.

The figure 6.46 shows also that with the VALKIN code it has been obtained a good qualitative reproduction of the reference power trend but quantitatively the results are not satisfactory, neither updating the mode each time step.

The reason of this disagreement is not known, probably have numerical origin; for the moment, only hypotheses can be advanced. In fact the practice to use the cross-sections carried out with RELAP5/PARCS calculations to perform VALKIN calculations it is a new procedure, used for the first time in this work.

Moreover, in order to analyze the influence of the number of modes on the results, it has been performed also a VALKIN calculation with 3 modes.

It has been possible only make a transient without update the modes because the updating process in this transient proves to be too expensive from the computational point of view.

As expected (the calculations with one mode have been already demonstrated that is necessary to update the modes each time step to carry out meaningful results), this calculation has not produced reliable results (see figure 6.47).

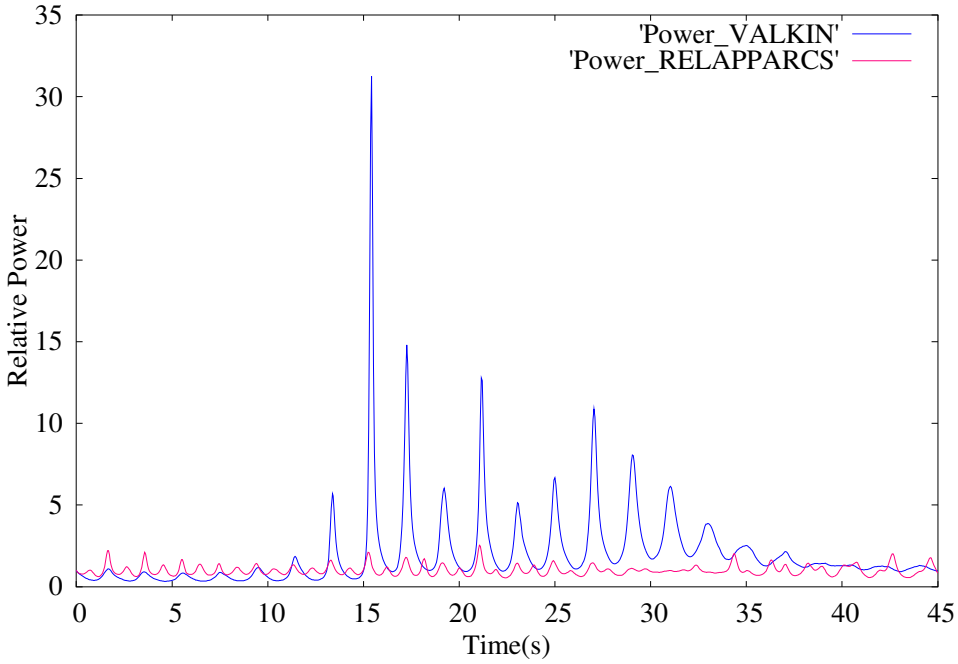

Figure 6-47: Comparison between the power evolution obtained with RELAP5/PARCS and the power evolution obtained using VALKIN code with 3 eigenvalues without updating the process.

Since it has been impossible to obtain meaningful information on the amplitude evolutions of the several modes with the power modal decomposition, the results of the precedent calculations have been complemented with a modal decomposition of the neutronic power from the local power distribution in the reactor core (provided by the simulation of the LPRM signals by RELAP5/PARCS).

As explicated in the section 6.3.1, the modal decomposition can be carried out considering only the signals from one of the axial levels LPRM's (specifically the signals of the LPRM located at the axial Level B).

The results obtained for the amplitude evolutions associated with the fundamental mode (N0) and with two azimuthal modes (N1 and N2) are shown in figure 6.48.

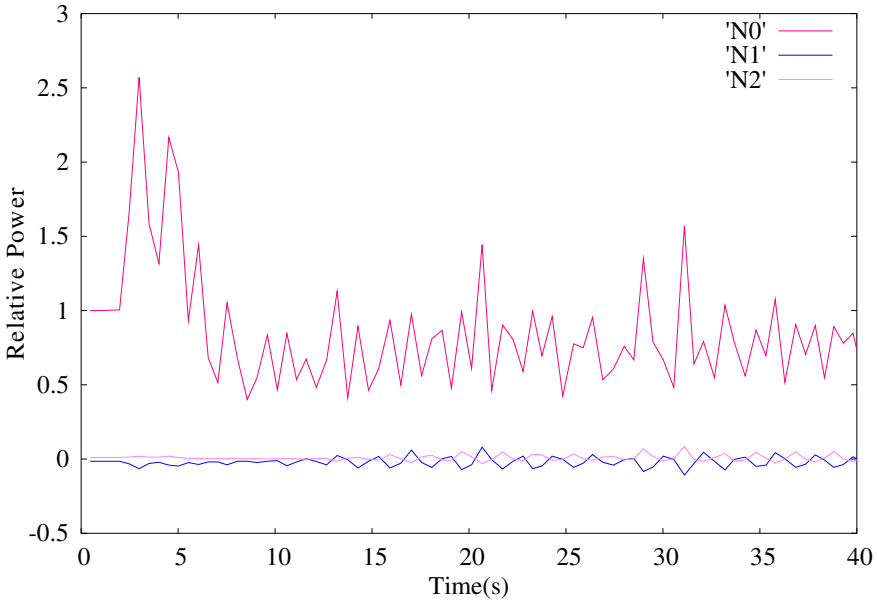

Figure 6-48: Amplitude evolutions obtained from the LPRM signals for case C1

In this case the amplitude of the azimuthal modes are not negligible so an association between an in-phase oscillation and two out-of-phase oscillations can be recognized.

Figure 6.49 represents the comparison among the fundamental amplitude and the power evolution provided by the RELAP5/PARCS transient calculation.

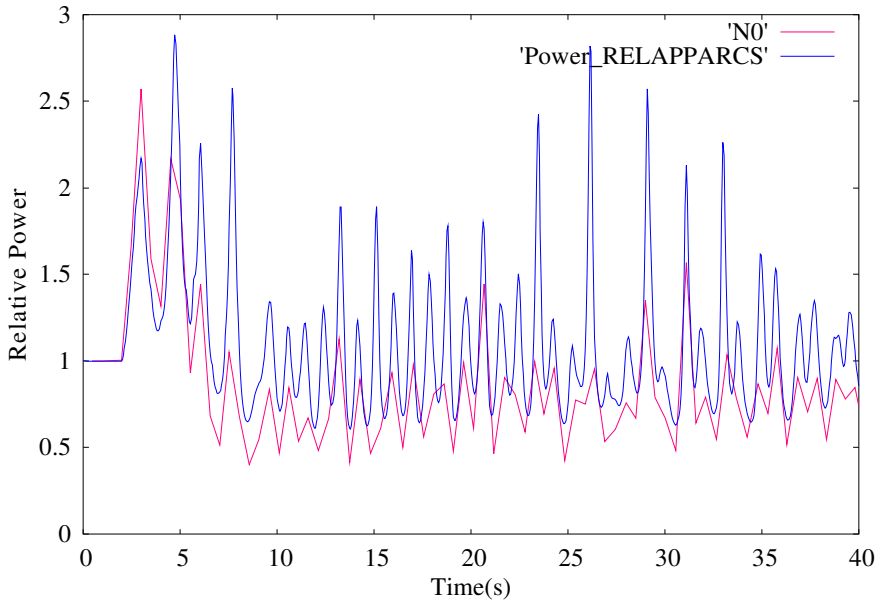

Figure 6-49: Comparison between the amplitude evolution associate with the fundamental mode and the power trend achieved with the RELAP5/PARCS calculation

It is noticeable as, only considering the signals from a small part of LPRM's (43 LPRM's) it is possible to achieve the same qualitative information obtained from the detailed nodal analysis where it is necessary to know the power distribution for all the reactor nodes (23712 nodes) at each time step.

The quantitative dissimilarity between the results can be reduced simply considering all the LPRM signals, but these type of analysis is made above all with the aim to obtain qualitative information on the unstable behaviour of the reactor and not to reproduce exactly its real behaviour.

Finally, a video clip of the evolution of the average power in the core during the first 50 seconds of the transient has been set up for this case. In the figure 50 some images of the video are reported. It is noticeable that with this 3-D representation additional information can be obtained about the nature of the oscillation: the video clip shows that though an in-phase oscillation is mainly involved, also an oscillation in the periphery of the reactor core appears, resulting in a rotation around the reactor centre.

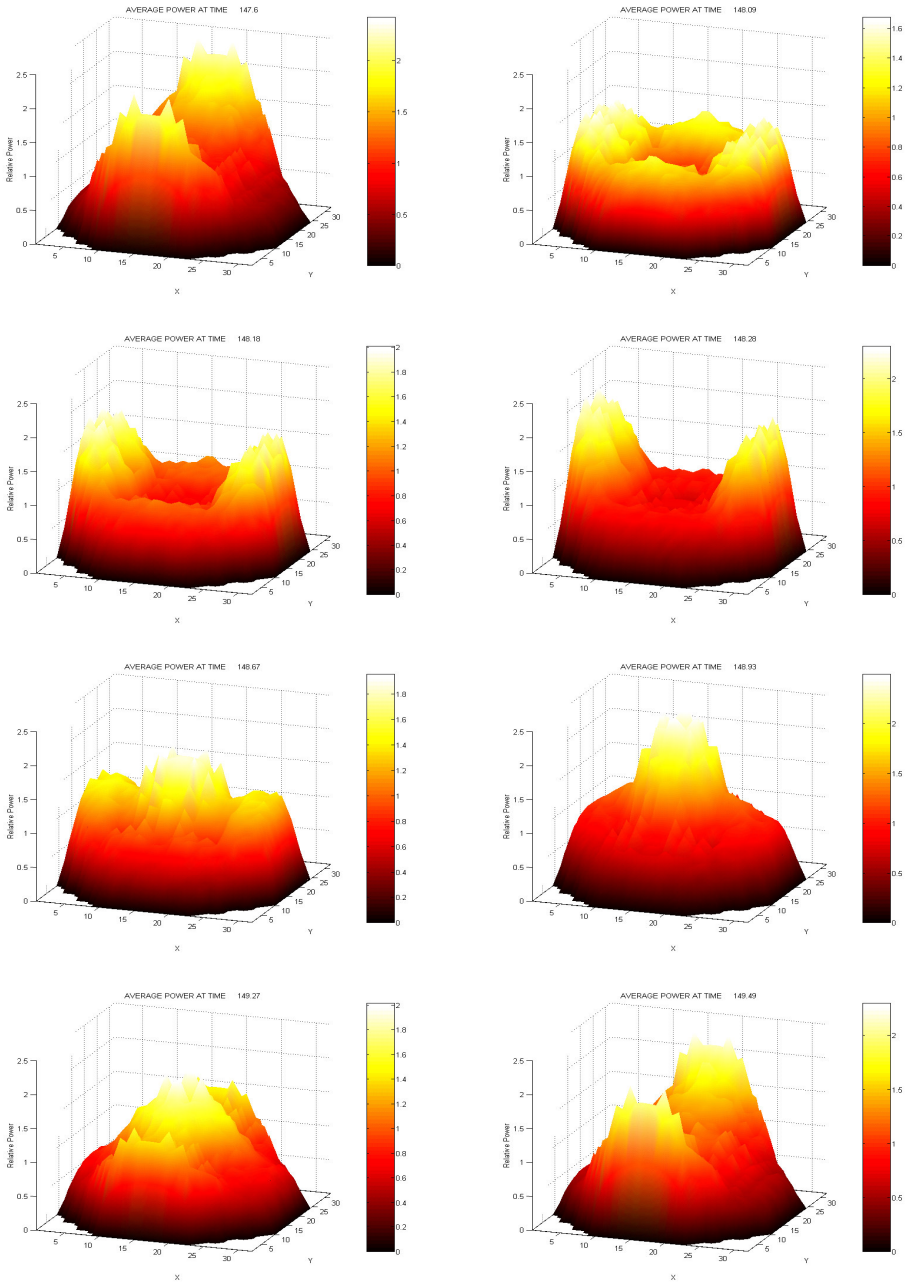

Figure 6-50: 3-D representations of the average power evolution during the transient time in case C1: from 147.7s to 149.7s

6.3.3.2 Case C2: Two Peaks Pressure Perturbation with a modified axial power distribution (model with 1 core channel)

A transient calculation similar to the one analyzed in the previous section has been performed with the couples codes RELAP5/PARCS, using the thermalhydraulic nodalization that with a single core channel: as

in the previous case. The axial power profile is changed at the beginning of the transient; then, the reactor is perturbed with a two peak steam line pressure perturbation.

As result of the new axial profile, plotted in figure 6.51, the reactor reaches a new stable condition: the core inlet flowrate drops 230 kg and the reactor power 100 MW.

In the figure 6.52, 6.53, 6.54 the core power, the core inlet mass flow rate and steam line pressure evolution calculated by the coupled codes are reported.

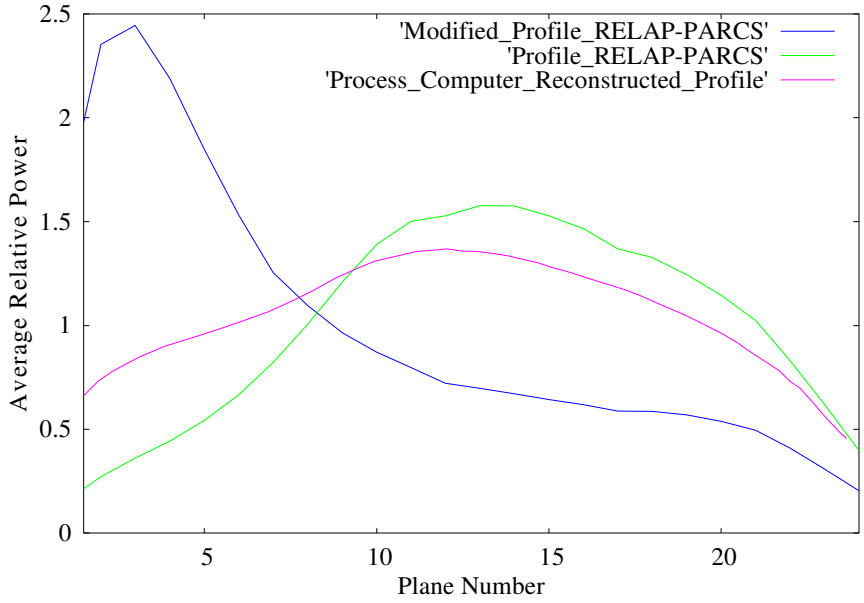

Figure 6-51: Comparison between the axial power distributions calculated before and after the control rod movement in case C2 and the reference one

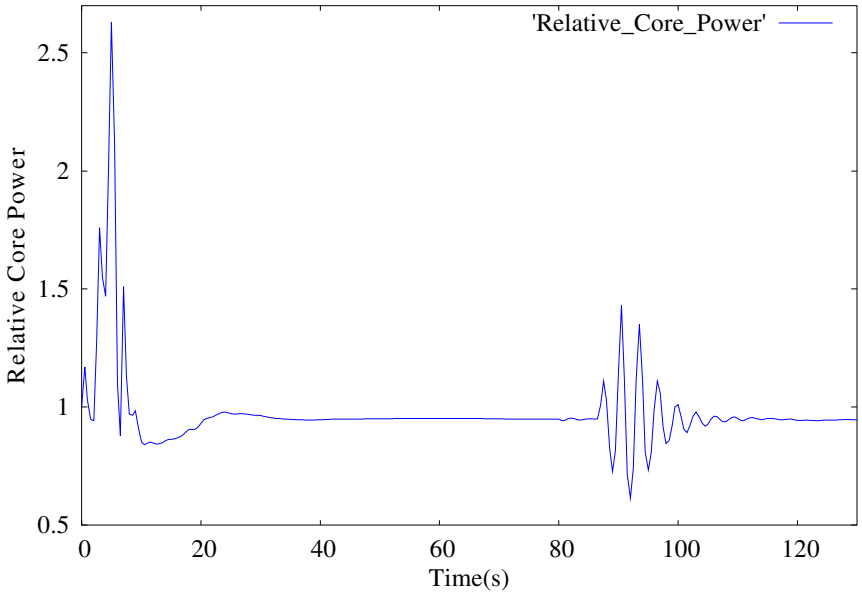

Figure 6-52: Reactor core power history during the transient in case C2

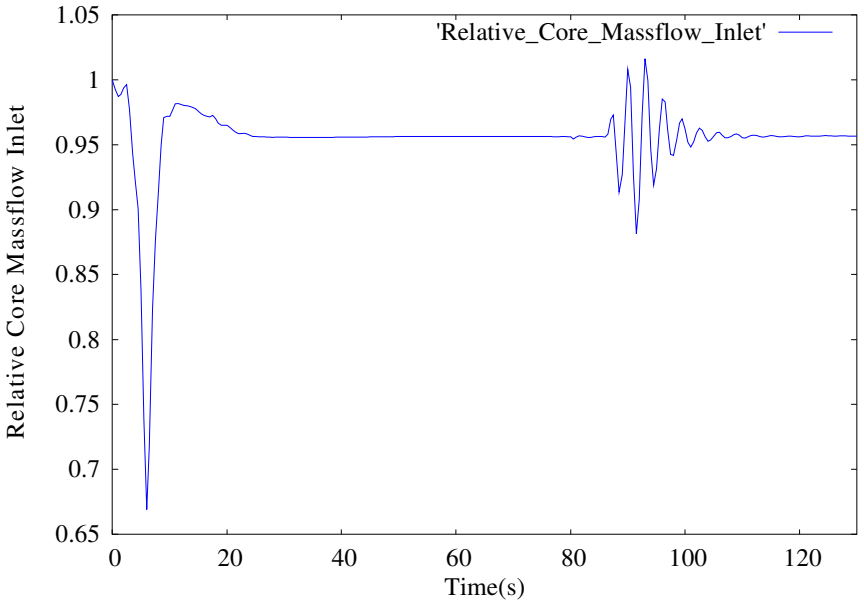

Figure 6-53: Core inlet mass flow rate during the transient in case C2

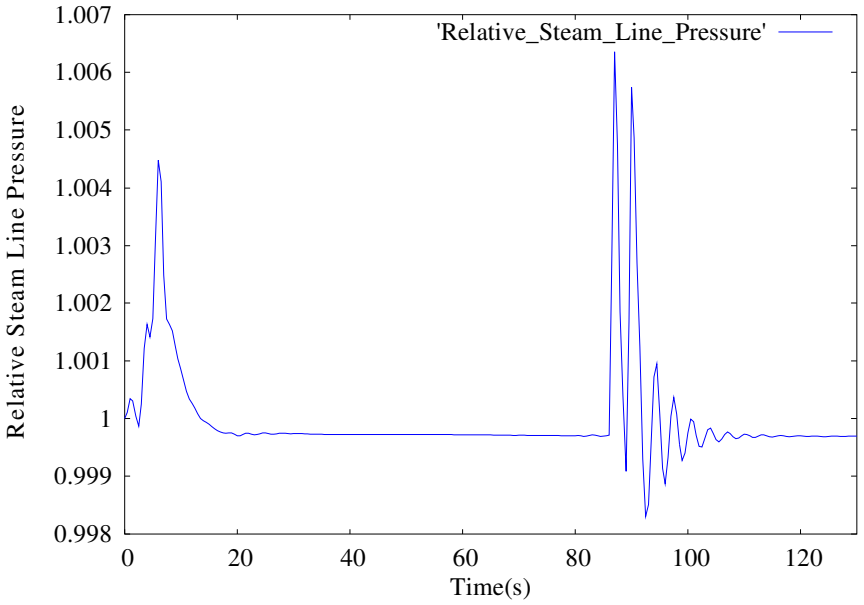

Figure 6-54: Steam line pressure history during the transient in case C2

In this case, the system does not develop unstable behaviour as a consequence of the disturbance in the steam line, that begins at 86 s and ends at 91 s; in fact, after the end of the perturbation, the oscillation is damped and the reactor tends to the new steady state conditions as the time simulation advances.

The following figures illustrate this behaviour.

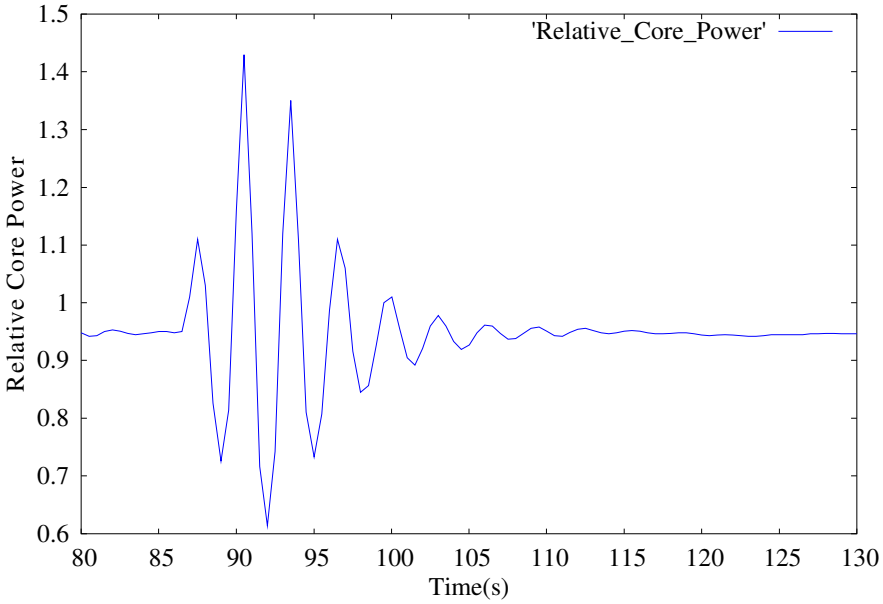

Figure 6-55: Reactor core power evolution during the perturbation in case C2

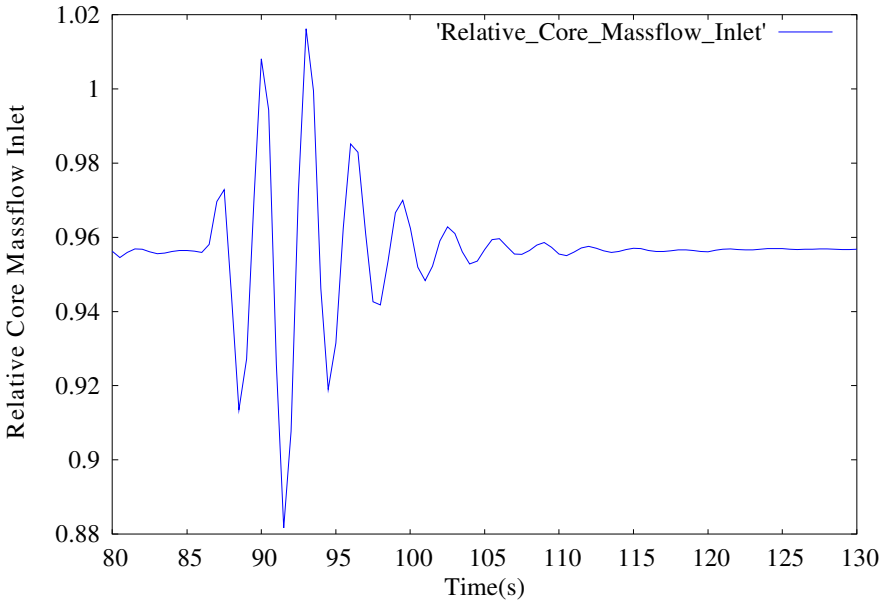

Figure 6-56: Core inlet mass flow rate evolution during the perturbation in case C2

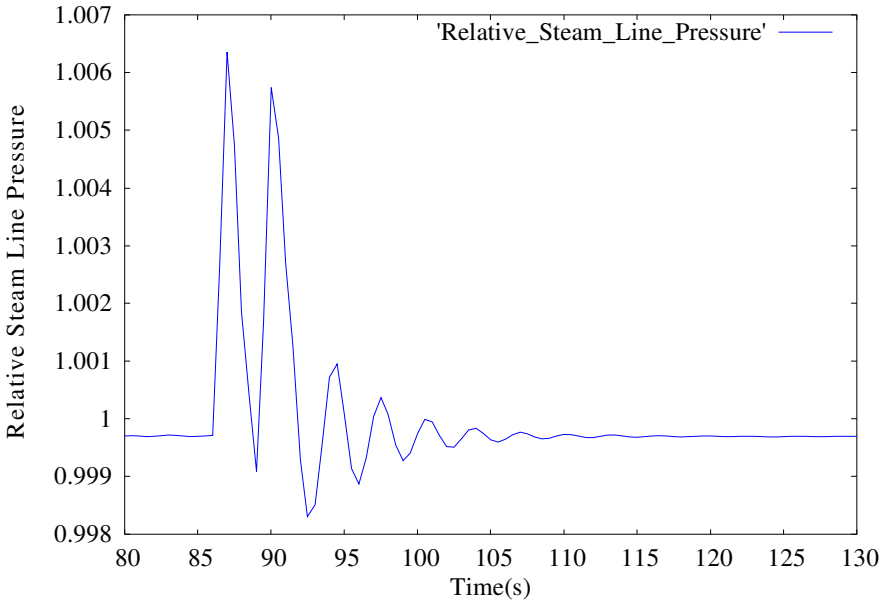

Figure 6-57: Steam line pressure evolution during the perturbation in case C2

As usual, it was also performed an analysis with the VALKIN code using the nuclear cross-sections achieved in the RELAP5/PARCS calculation.

Two tests were performed, without and with updating of the cross sections; in both the cases only one mode was used.

In the next figures (figures 6.58 and 6.59) the effects on the power trend of the steam line pressure disturbance as simulated by the VALKIN code and by the coupled codes RELAP5/PARCS are reported.

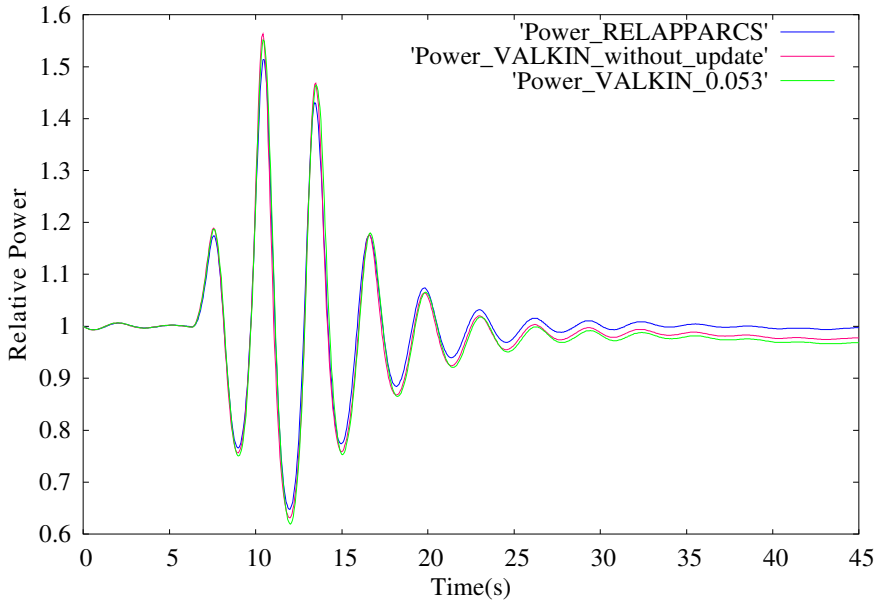

Figure 6-58: Comparison between the power evolution obtained with RELAP5/PARCS and the power evolution obtained using VALKIN code with 1 eigenvalue and different updating times.

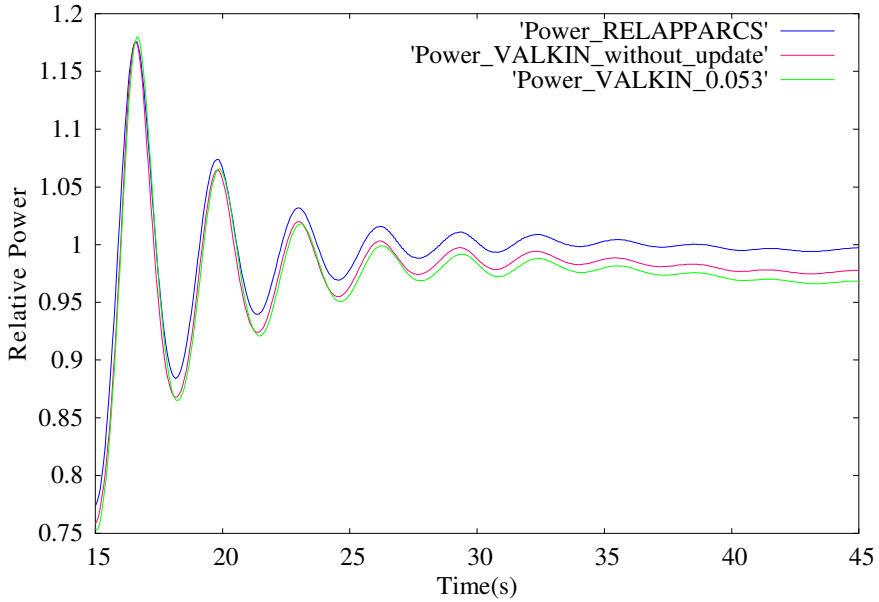

Figure 6-59: Particular of the comparison represented in the previous figure

The figures show the good agreement between the results achieved with the two different codes: at the end of the transient calculation, where the solutions seems more dissimilar, the deviation between the results is still negligible (about 0.01%for the power).

Observing the maxima and minima of the oscillations, it is noticeable the improvement of the solution as a consequence of the adoption of the updating strategy.

6.3.3.3 Case C: Two Peaks Pressure Perturbation with a modified axial power distribution (comparison between the results achieved with the two different nodalizations)

In this section the results obtained analyzing the same test (case C) with the RELAP5/PARCS coupled codes by the two different thermalhydraulic models are discussed.

The first three figures report the effect of the control rod movement in the two analyses; the subsequent figures describe the consequences of the steam line pressure perturbations on the system in the two simulations.

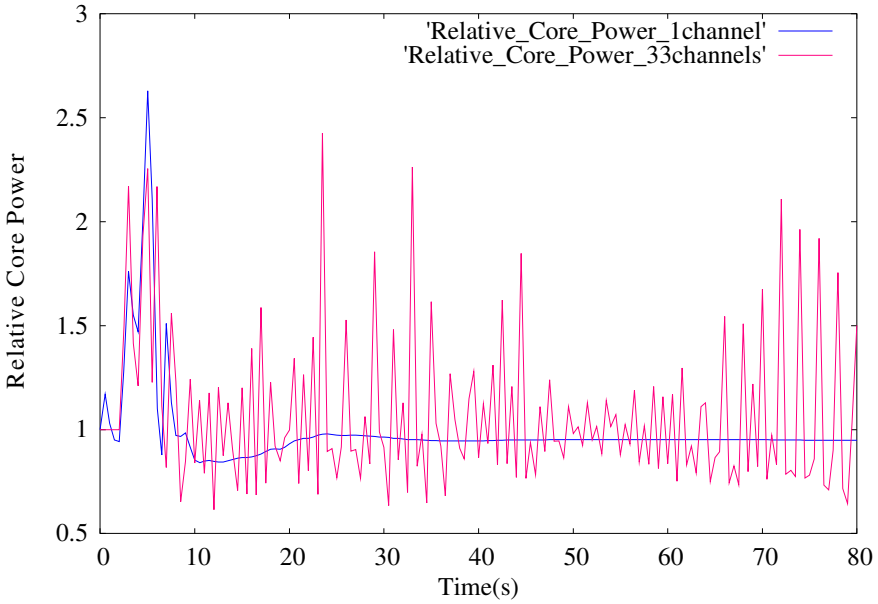

Figure 6-60: Control rod movement comparison between the core power evolutions obtained with the two different thermalhydraulic models in case C

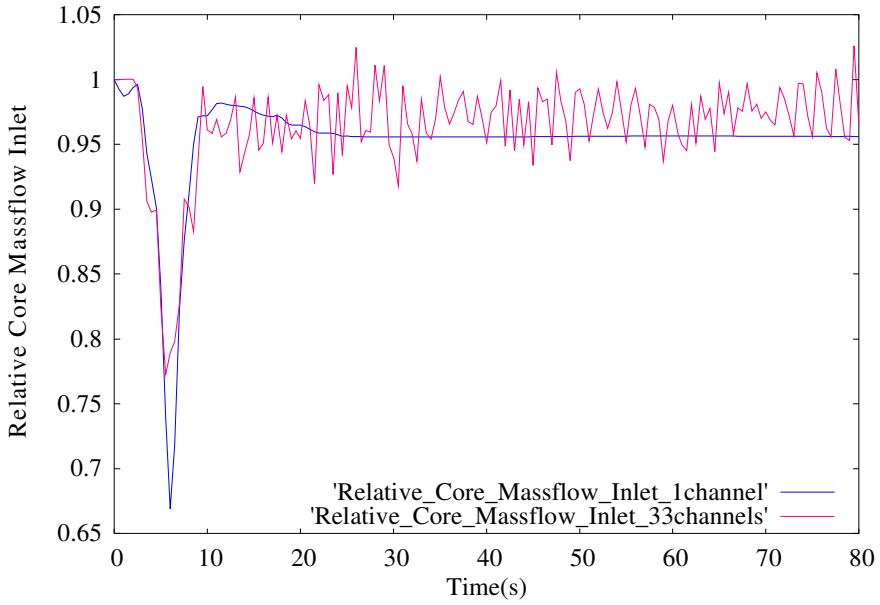

Figure 6-61: Control rod movement comparison between the core inlet mass flow rate evolutions obtained with the two different thermalhydraulic models in case C

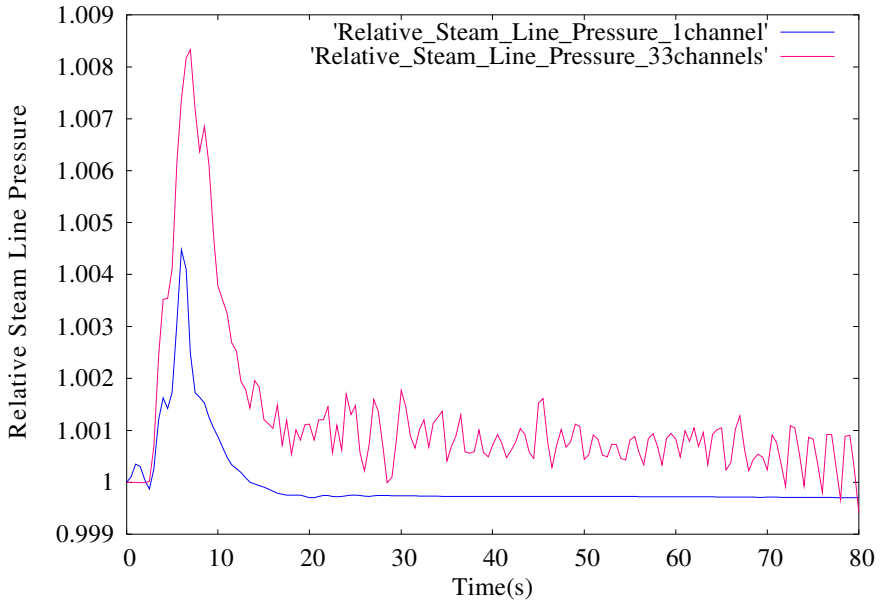

Figure 6-62: Control rod movement comparison between the steam line pressure evolutions obtained with the two different thermalhydraulic models in case C

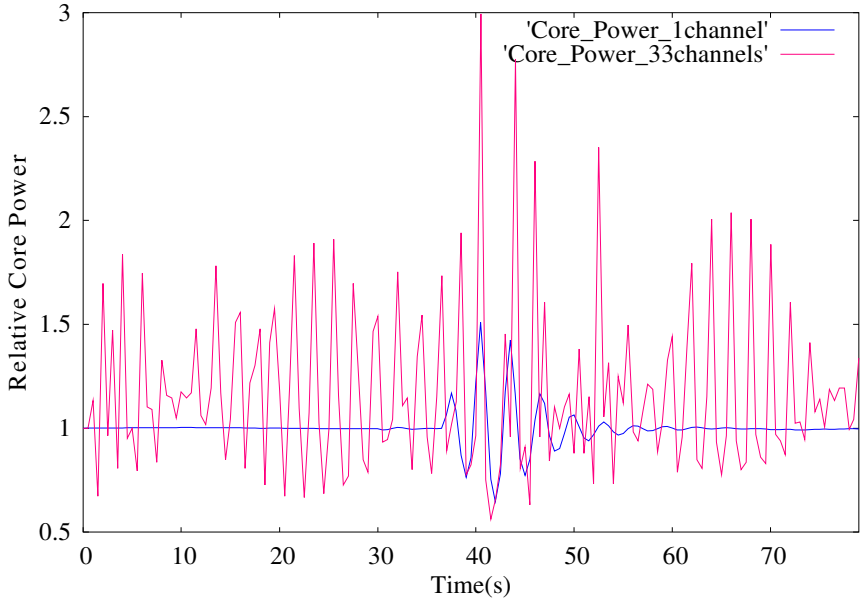

Figure 6-63: Comparison between the core power evolutions obtained with the two different thermalhydraulic models in case C during the disturbance

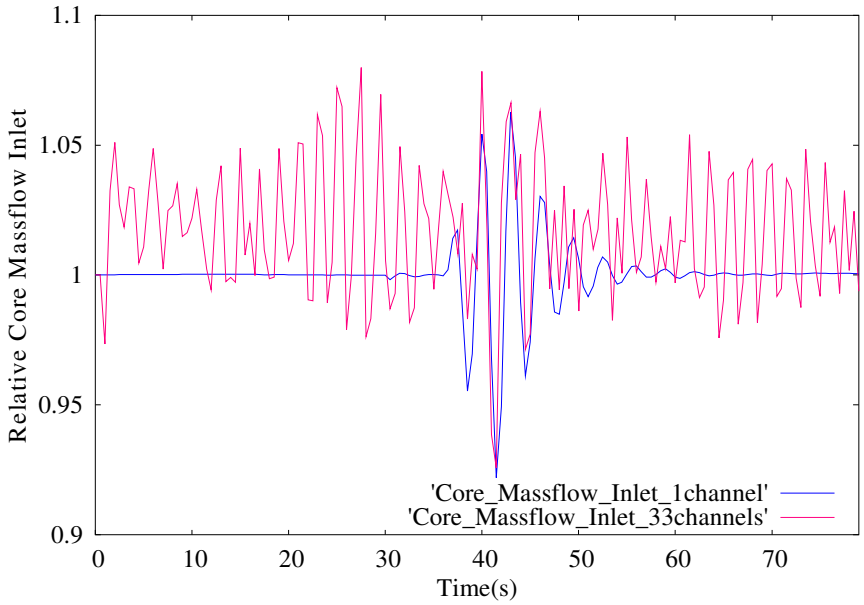

Figure 6-64: Comparison between the core inlet mass flow rate evolutions obtained with the two different thermalhydraulic models in case C during the disturbance

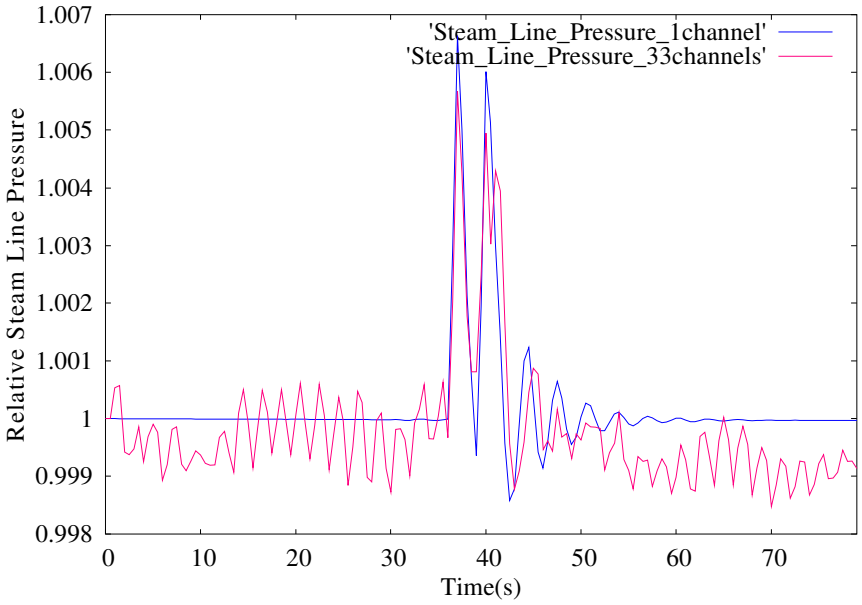

Figure 6-65: Comparison between the steam line pressure evolutions obtained with the two different thermalhydraulic models in the Case C during the disturbance

In both the cases the pressure disturbance in the steam line does not produce any effect on the system; nevertheless it appears clearly from the figures that for this perturbation the solutions obtained with the two models are completely different. In the analysis performed with the single channel core model the system does not develop an unstable behaviour and the change in the axial power shape produces only a change in the reactor steady conditions; on the contrary, with the more complex nodalization a self-sustained unstable behaviour is observed.

6.3.4 Oscillation analysis: Decay Ratio and Natural Reactor Frequency calculation and analysis of the LPRM signals

The following table summarizes and compares with the reference data the calculated Natural reactor Frequency and Decay Ratio for the considered cases

Table 6-2. Time series analyses results

	DR	Frequency
Reference	0.331	0.430
Case A1 (two peaks SL pressure perturbation, 33channels T/H core model)	0.299	0.316
CaseA2 (two peaks SL pressure perturbation, 1channel T/H core model)	0.400	0.3014
CaseB1 (Pseudo Random SL pressure perturbation, 33channels T/H core model)	0.336	0.3043
Case B2 (Pseudo Random SL pressure perturbation, 1 channel T/H core model)	0.347	0.298
Case C1 (modified axial power distribution, two peaks SL pressure perturbation, 33channels T/H core model)	0.985	0.518
Case C2 (modified axial power distribution, two peaks SL pressure perturbation, 1channel T/H core model)	0.498	0.316

It is clear from the table that the calculated values are in the same range of the reference data (except for case C, which represents a considerably different condition), though quantitative discrepancies are observed.

Concerning the differences between the frequencies achieved for the several cases, it is evident from the figures of the previous sections that in all cases analyzed the system oscillates in a different way. Nevertheless, interesting conclusions can be achieved observing the frequency values: in all the oscillations, go from about 0.3 to approximately 0.5, i.e., in the typical frequency range of the in-phase instability event.

Finally, signals of LPRM located in opposite reactor zones, simulated in the RELAP5/PARCS transient calculations, have been compared (see following figures).

In the figure 6.66 the LPRM are represented the position of the LPRM in the core with black point. Dividing the core in quarters, the signals of LPRM's located in each quarter have been confronted against the others.

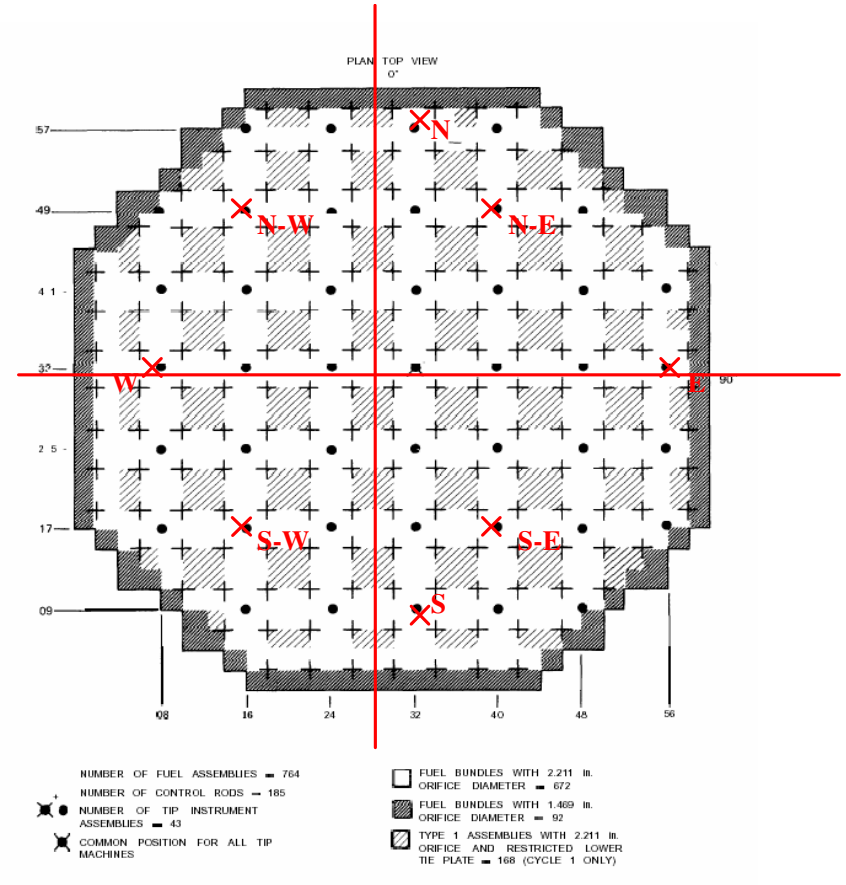

Figure 6-66 LPRM system arrangement

The 4 axial levels of LPRM's (Level A, Level B, Level C, and Level D) are axially located from bottom to top of the active fuel length at 45.7, 137.2, 228.6, and 304.8 cm respectively (see figure 3.7); the signals plotted in the following figures are provided by the LPRM located at Level B.

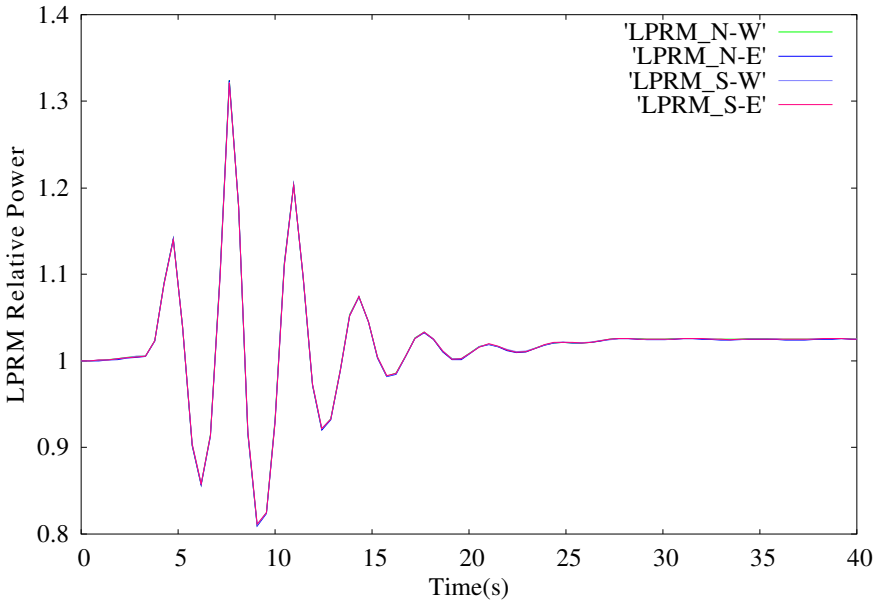

Figure 6-67: Comparison between opposite LPRM signals in case A1

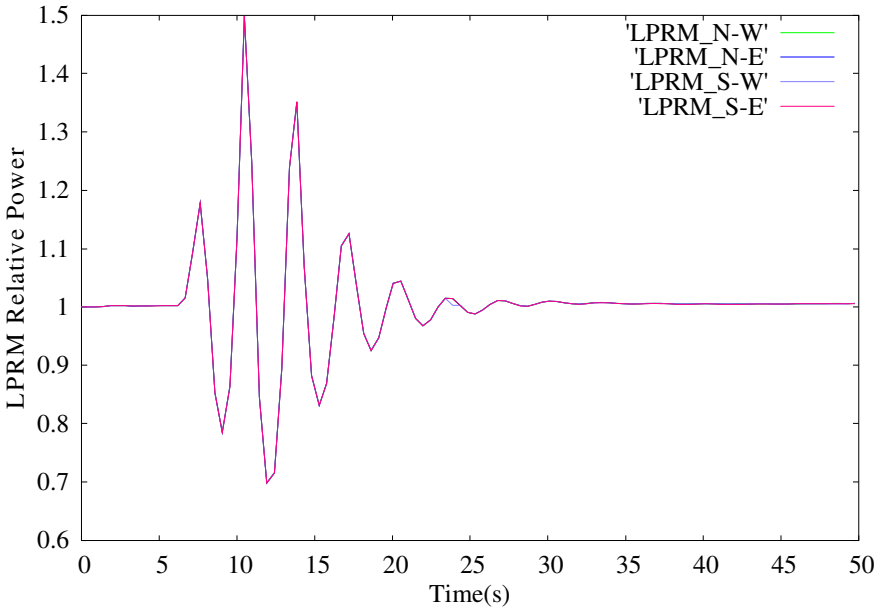

Figure 6-68: Comparison between opposite LPRM signals in case A2

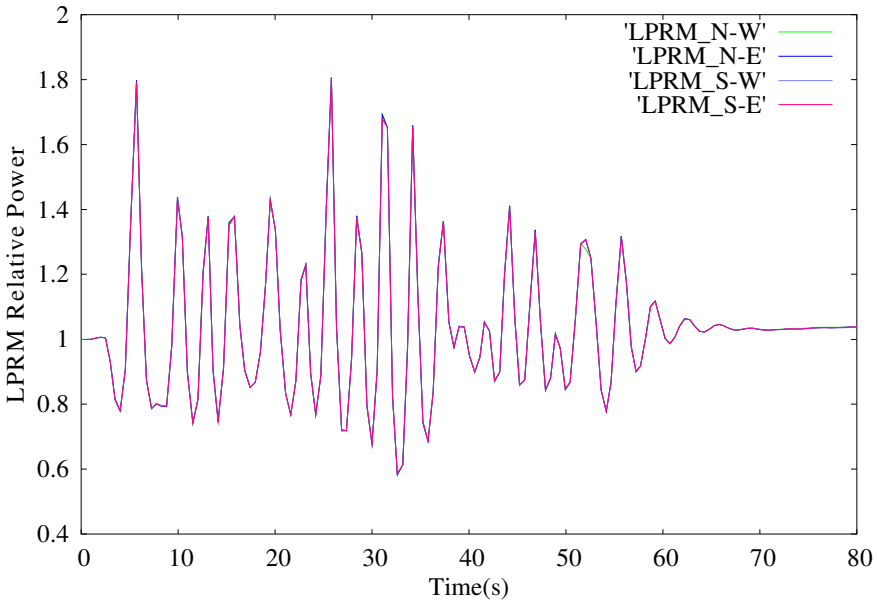

Figure 6-69: Comparison between opposite LPRM signals in case B1

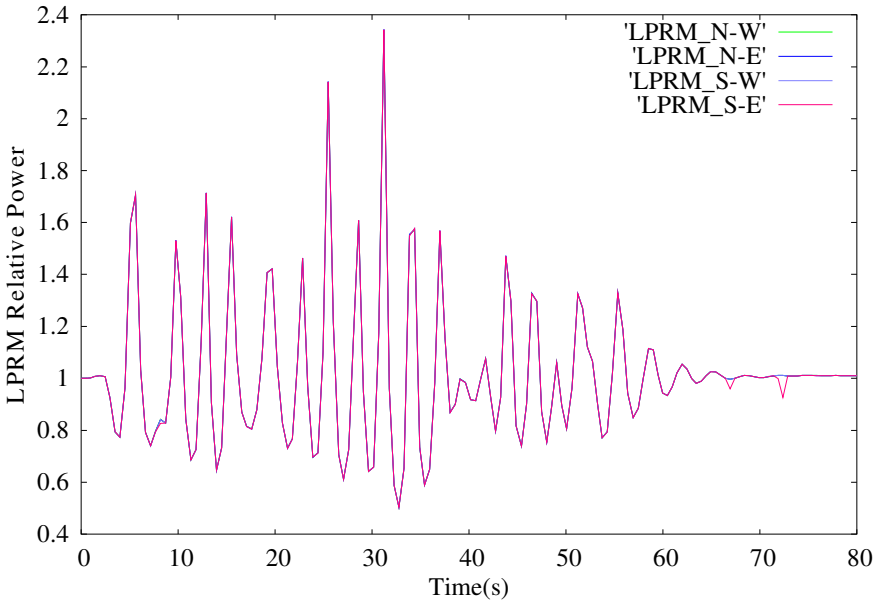

Figure 6-70: Comparison between opposite LPRM signals in case B2

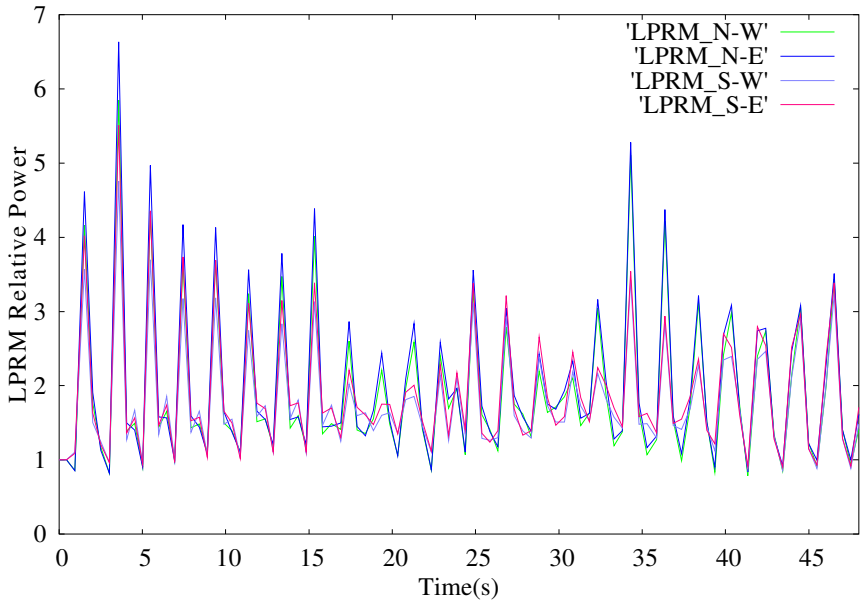

Figure 6-71: Comparison between opposite LPRM signals in case C1

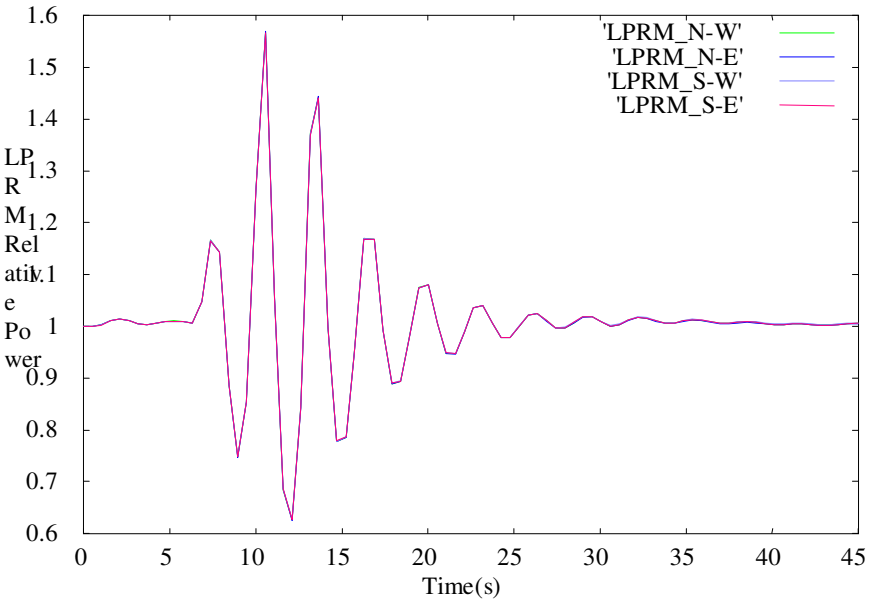

Figure 6-72: Comparison between opposite LPRM signals in case C2

In all the comparisons it is evident that the system develops in-phase instabilities; in fact the evolution of the signals provided by the different LPRM during the transients is always practically the same. These results reveal a good agreement between simulated and real behaviour of the Peach Bottom-2 reactor, in which only in-phase instabilities were observed.

Hence, analyzing the frequency values and the LPRM signals trends in the different cases it is possible to recognize characteristics of the in-phase instability although, experimentally, the Point 3 of the Peach Bottom-2 Low Flow Stability Tests (chosen as actual test conditions in all the analyses performed) appears a nearly stable point.

In addition, the signals of the LPRM's north (N), south (S), west (W) and east (E) have been reported for case C1.

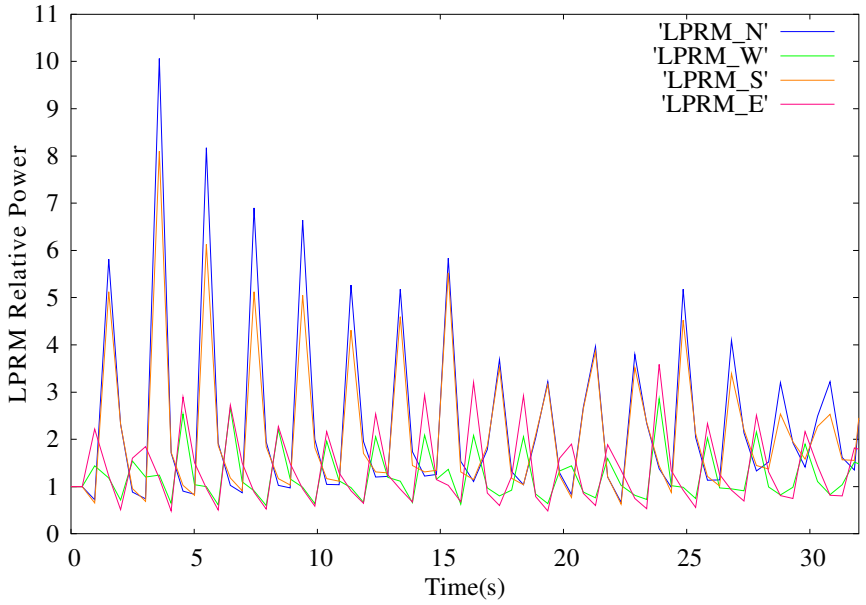

Figure 6-73: Comparison between opposite LPRM signals in case C1

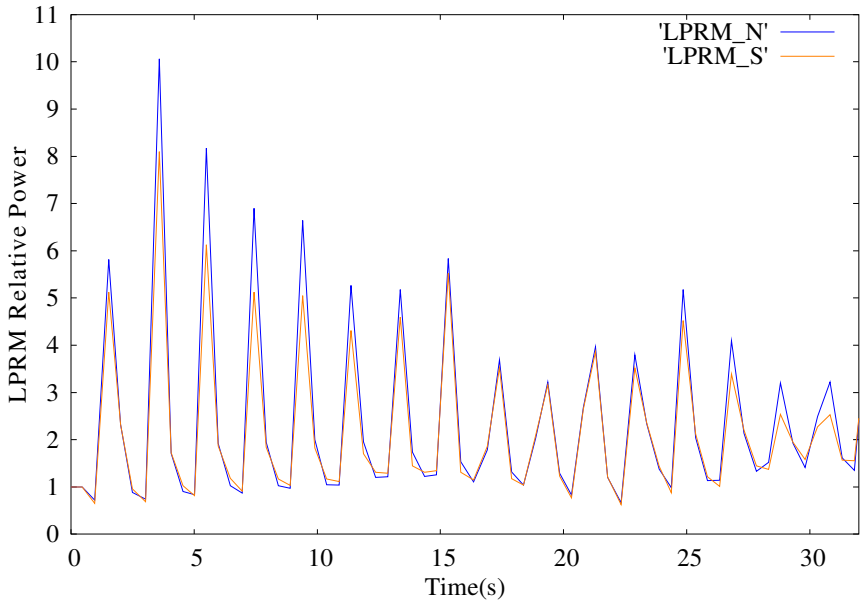

Figure 6-74: Comparison between opposite LPRM signals (LPRM north and south) in case C1

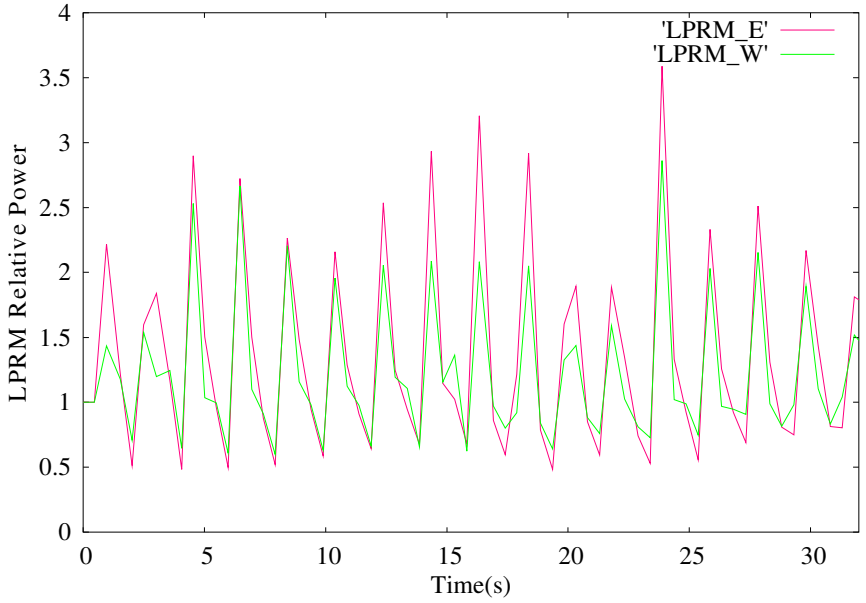

Figure 6-75: Comparison between opposite LPRM signals (LPRM east and west) in case C1

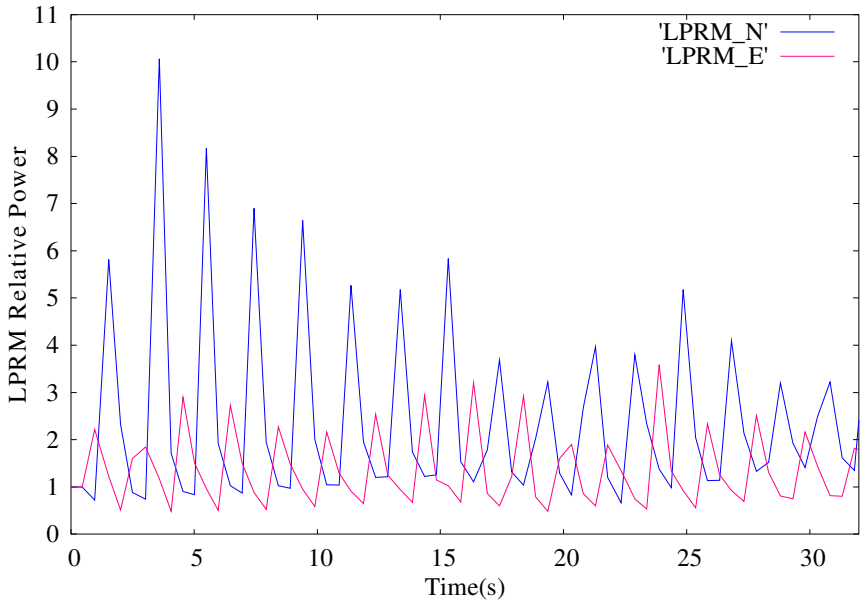

Figure 6-76: Comparison between opposite LPRM signals (LPRM north and east) in the Case C1

It is noticeable that the north and south halves oscillate in-phase analogously to the halves east and west, while adjacent halves oscillate with a phase shift of 180°. So, also with this tool, the same behaviour of the oscillation discovered with the video clip has been recognized, i.e., the external average power oscillation rotates around the centre of the core during the transient.

6.4 COMPARISON BETWEEN THE OBTAINED RESULTS WITH TWO DIFFERENT THERMALHYDRAULIC-NEUTRONIC COUPLED CODES

In the aim to better understand the instability development process and in order to compare the solutions obtained with two different thermalhydraulic and neutronic coupled codes, the analysis of case A1 has been performed employing different coupled codes, namely the TRAC/BF1-VALKIN codes.

6.4.1 TRAC/BF1-VALKIN code

TRAC/BF1-VALKIN code is a time-domain analysis code conceived to study transients in a BWR reactor. This code uses the best estimate code TRAC/BF1 to account for the heat transfer and thermalhydraulic processes and

the already mentioned 3-D neutronics module VALKIN (see section 4.4 for the VALKIN code description).

The thermalhydraulic code TRAC/BF1 [31] uses a two fluids, six-equation model to simulate the thermalhydraulic phenomena. The coupled code has been called TRAC/BF1-VALKIN and it can be used to simulate plant transients considering the neutronic phenomena in 3-D geometry and the thermalhydraulic processes in multiple-channel 1-D geometry.

6.4.1.1 TRAC/BF1-VALKIN coupling

The TRAC/BF1 code [31] has models for the usual components of a BWR reactor as the vessel, channels, pumps, separators-dryers, etc. The fuel channels in the core are modelled with multiple channels components. To model the heat transfer in the fuel, an axial-radial heat transfer algorithm is used. The thermalhydraulic processes are modelled solving six balance equations of mass, momentum and energy for the liquid and the vapour phases. For the numerical integration of the fluid flow equations a semi-implicit two step method is used for the time discretization, and a first order finite difference method with staggered mesh is applied to discretize the spatial part of the equations.

The nuclear cross-sections associated to each neutronic node are obtained interpolating the values of multiple entry tables in terms of the thermalhydraulic variables and the control rods insertion pattern. These nuclear cross-sections are used to obtain the power distribution with VALKIN module. This power distribution is used as an input for TRAC/BF1 in the POST stage [31] to obtain the thermalhydraulic variables, which are used to obtain a second set of cross-sections. Then, TRAC/BF1 uses the nodal power distribution provided by VALKIN in the PREP and OUTER stages. Both sets of cross-sections are used for the implicit integration of the nodal equations by the VALKIN code. The cross-sections at intermediate time steps are obtained by linear interpolation from both sets of cross-sections. In this way, an explicit coupling between VALKIN and TRAC/BF1 codes is obtained, performed in a sequential way and allowing the use

of different time steps for the internal neutronic calculations and the thermalhydraulic calculations.

6.4.2 Transient Description and thermalhydraulic and neutronic modeling

With the TRAC-BF1/VALKIN coupled codes exactly the same analyses performed with the RELAP5/PARCS for case A1 were performed; (for more information on the test conditions, see section 5.1).

A detailed thermalhydraulic nodalization has been developed reproducing each geometrical zone of the plant [32]: 33 thermalhydraulic channels have been modelled to represent the active part of the core and one channel for simulating the bypass. The rest of the plant has been represented by a coarse nodalization in order to limit the needed computer resources.

For the neutronic code, a nodalization with a 3-D core mesh composed with 764 axial nodes has been adopted. A large set of cross-section data including 435 compositions has been adopted in the neutronic input deck [13].

The core neutronic data used in all the calculations are specified in [16].

Two different calculations have been performed, the first (case 1) without updating the mode, and the second (case 2) updating the mode with a period of 1 s.

6.4.3 Comparison of results

6.4.3.1 Steady state results

The following table presents the main reactor parameters (reactor power, reactor mass flow rate inlet, feedwater mass flow rate, core exit pressure, core inlet temperature and core inlet enthalpy) prior to its disturbance for the two calculations performed and their comparison with available measured data.

Table 6-3- Reactor main parameters prior to its disturbance

Parameters, Units	Measured	RELAP5/PARCS (33 channels)	TRAC-BF1/VALKIN (33 channels)
Core thermal power, MWt	1948.0	1949.0	1949.0
Reactor flow, kg/s	5216.40	5216.332	5212.6
Core inlet temperature, K	543.16	543.014	541
Core inlet enthalpy, J/kg	1.1846E6	1.1839E6	1.1741E6
Pressure at core outlet, Pa	7.0980E6	7.0979E6	7.035E6
Feedwater massflow, kg/s	941.22	941.22	941.10

Figure 6.77 compares the core average axial power distribution simulated with the codes, with the reference one.

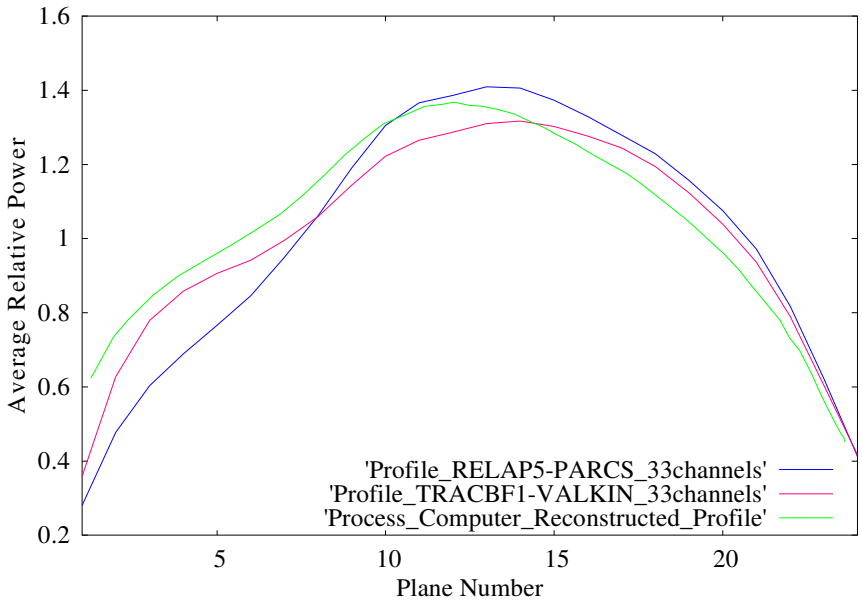

Figure 6-77 Comparison of RELAP5/PARCS and TRAC-BF1/VALKIN calculated core average axial power distributions with experimental test (process computer corrected).

6.4.3.2 Transient results

Table 6.4 presents a comparison between the Decay Ratio and the Natural Reactor Frequency calculated with the two different coupling codes and the reference data:

Table 6-4 Time series analyses results

	DR	Freq.
Reference	0.331	0.430
TRAC/VALKIN case 1	0.4172	0.3032
TRAC/VALKIN case 2	0.4883	0.3097
RELAP5/PARCS	0.299	0.316

Finally, figure 6.78 compares the results obtained with RELAP5/PARCS and TRAC/VALKIN, using only one mode, without updating (case 1) and with updating (case 2). A relatively good agreement between RELAP5/PARCS and TRAC/VALKIN is observed with the updating strategy also with the TRACB/F1-VALKIN coupled codes.

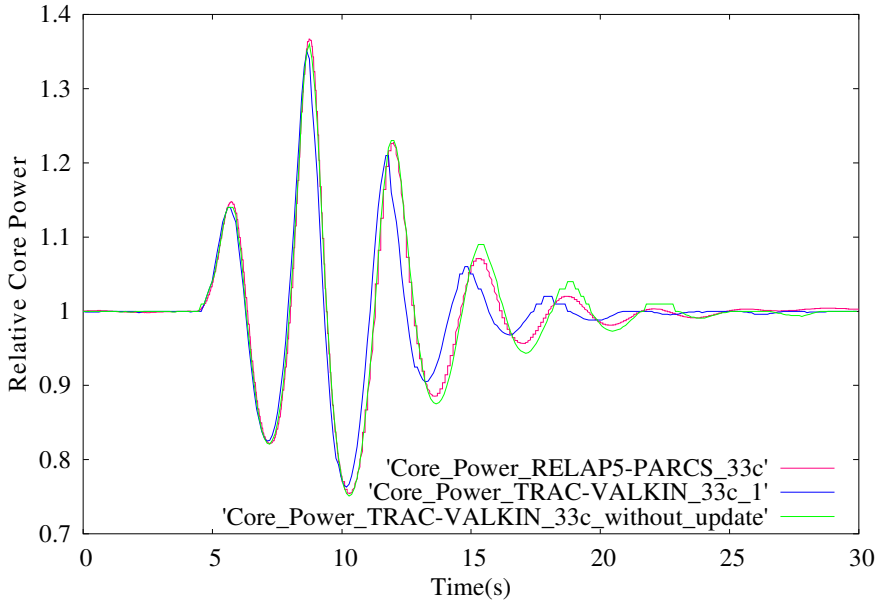

Figure 6-78: Comparison between RELAP5/PARCS and TRAC/VALKIN with no update and with updating time of 1 second.